An inducible ER–Golgi tether facilitates ceramide transport to alleviate lipotoxicity

Li-Ka Liu, Vineet Choudhary, Alexandre Toulmay,* and William A. Prinz*

Laboratory of Cell and Molecular Biology, National Institute of Diabetes and Digestive and Kidney Diseases, National Institutes of Health, Bethesda, MD 20892

Ceramides are key intermediates in sphingolipid biosynthesis and potent signaling molecules. However, excess ceramide is toxic, causing growth arrest and apoptosis. In this study, we identify a novel mechanism by which cells prevent the toxic accumulation of ceramides; they facilitate nonvesicular ceramide transfer from the endoplasmic reticulum (ER) to the Golgi complex, where ceramides are converted to complex sphingolipids. We find that the yeast protein Nvj2p promotes the nonvesicular transfer of ceramides from the ER to the Golgi complex. The protein is a tether that generates close contacts between these compartments and may directly transport ceramide. Nvj2p normally resides at contacts between the ER and other organelles, but during ER stress, it relocalizes to and increases ER–Golgi contacts. ER–Golgi contacts fail to form during ER stress in cells lacking Nvj2p. Our findings demonstrate that cells regulate ER–Golgi contacts in response to stress and reveal that nonvesicular ceramide transfer out of the ER prevents the buildup of toxic amounts of ceramides.

Introduction

Several critical lipid intermediates, such as DAG and ceramide, can be toxic when they accumulate in cellular membranes. This is not only because they affect membrane structure and organization but also because they are potent signaling molecules. Numerous studies have linked elevated ceramides with cellular stress, cell cycle arrest, apoptosis, and insulin resistance; ceramide accumulation is also associated some cancers and neurodegenerative diseases (Xie et al., 1998; Holland et al., 2007; Pickersgill et al., 2007; Ledeen and Wu, 2008; Bikman and Summers, 2011; Mullen and Obeid, 2012). Ceramide toxicity has also been demonstrated in *Saccharomyces cerevisiae* and may cause an apoptosis-like cell death (Eisenberg and Büttner, 2014).

How cells monitor ceramide levels and prevent the accumulation of excess ceramide is only partially understood. Ceramides are synthesized de novo in ER membranes by the *N*-acylation of sphingoid long-chain bases (LCBs) with fatty acids (Fig. 1 A; Merrill, 2002). They are also generated by degradation of complex sphingolipids. Ceramide levels are modulated by mechanisms in addition to regulating synthesis. Most cells possess several ceramidases, which hydrolyze ceramides into LCBs and fatty acids (Ito et al., 2014). There is also growing evidence that cells convert excess ceramides into other lipids to prevent the toxic accumulation of ceramides. For example, a sphingomyelin synthase-related protein in the ER generates a sphingomyelin analogue from ceramide (Ternes et al., 2009; Vacaru et al., 2009), and it has recently been found that this enzyme is necessary to prevent the toxic accumulation of ceramides and apoptosis (Tafesse et al., 2014). Another method for removing excess ceramide has been identified in yeast. It has recently been found that ceramides can be converted into acylceramides, which are probably not toxic (Voynova et al., 2012).

How ceramides traffic in cells is only incompletely understood. After ceramides are synthesized in the ER, they are transferred to the Golgi complex, which is the location of the enzymes that generate complex sphinogolipids from ceramide. Ceramide transport from the ER to the Golgi complex occurs by both vesicular and nonvesicular mechanisms. Ceramide transport protein (CERT) facilitates nonvesicular ceramide transport in mammalian cells; cells that lack this protein have a significantly reduced rate of sphingomyelin formation (Hanada et al., 2003).

In *S. cerevisiae*, ceramides are also transported from the ER to the Golgi complex by both vesicular and nonvesicular pathways (Funato and Riezman, 2001). The nonvesicular pathway seems to be relatively minor in this yeast because mutations that block vesicular trafficking reduce ceramide transport by ∼80% (Funato and Riezman, 2001). *S. cerevisiae* lacks a CERT homologue, and it is not known how nonvesicular transport is facilitated. Once ceramides reach the medial-Golgi in

*A. Toulmay and W.A. Prinz contributed equally to this paper.

Correspondence to Alexandre Toulmay: toulmayal@niddk.nih.gov; or William A. Prinz: prinzw@helix.nih.gov

Abbreviations used: DHS, dihydrosphingosine; EGT, ER–Golgi tether; E-Syt, extended synaptotagmin; IPC, inositolphosphorylceramide; LCB, long-chain base; MBP, maltose-binding protein; MCS, membrane contact site; NVJ, nucleus vacuolar junction; PA, phosphatidic acid; PC, phosphatidylcholine; PE, phosphatidylethanolamine; PH, pleckstrin homology; PIP, phosphatidylinositol phosphate; SC, synthetic complete; SMP, synaptotagmin-like mitochondrial lipid-binding protein; TM, transmembrane; UPRE, unfolded protein response promoter element.

The Rockefeller University Press $30.00
J. Cell Biol. Vol. 216 No. 1 131–147
https://doi.org/10.1083/jcb.201606059

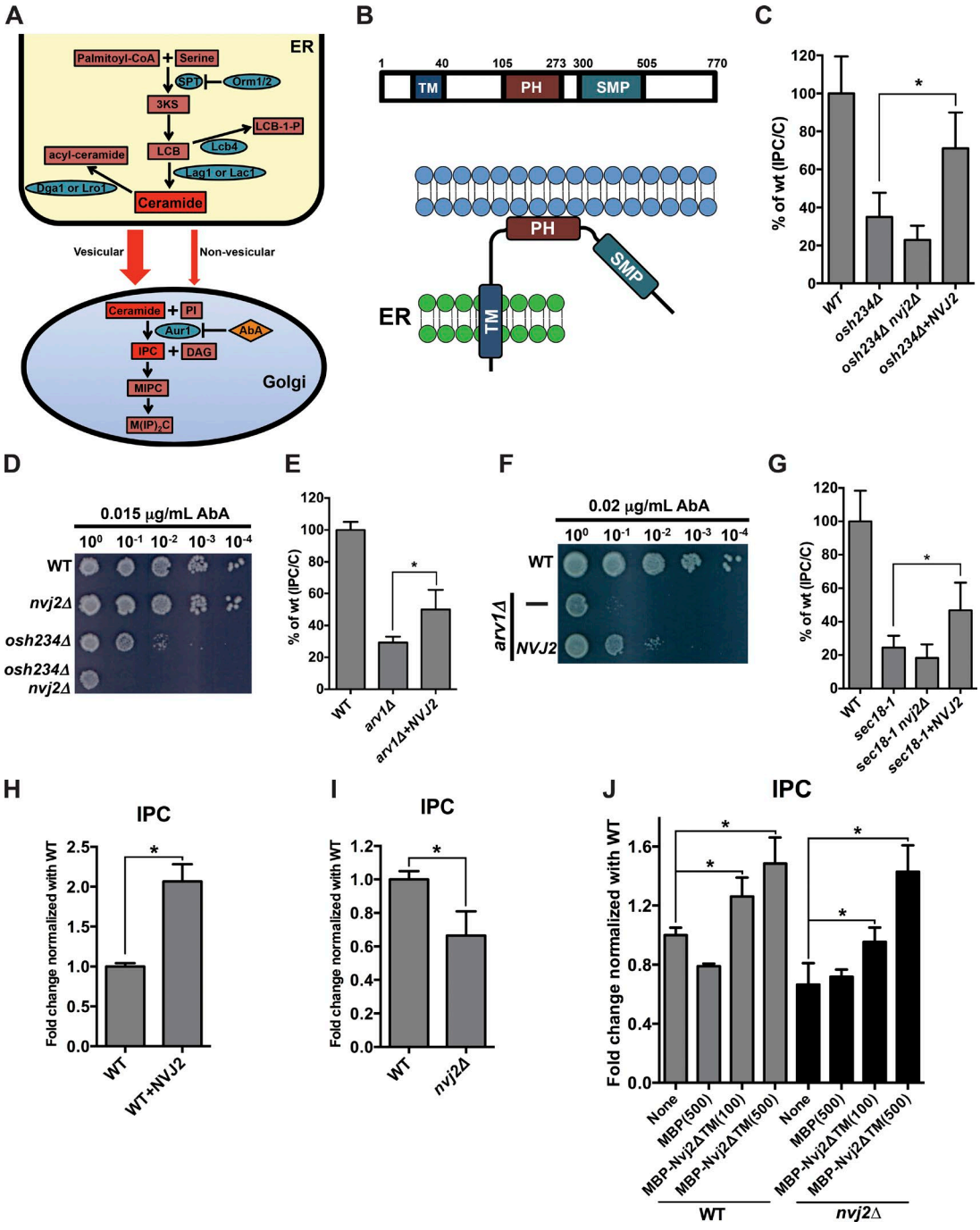

Figure 1. **Nvj2p facilitates nonvesicular ceramide transport.** (A) Diagram of sphingolipid metabolism and ceramide transport in *S. cerevisiae*. (B) Domains and putative topology of Nvj2p. Numbers indicate amino acids. (C and E) Cell were labeled with [^{3}H]serine for 1 h at 25°C and the relative IPC/C determined. Mean ± SD of three (C) or six (E) independent experiments. (D and F) Serial dilutions of strains grown on SC containing the indicated concentration of AbA. (G) As in C, except that cells were grown for 20 min at 25°C in SC medium with 200 µg/ml cycloheximide, shifted to 37°C for 30 min, and labeled with [^{3}H]serine for 30 min at 37°C. (H and I) Lysates from the indicated strains were labeled with [^{3}H]DHS for 2 h at 25°C, and the relative amount of radiolabeled IPC formed was determined. Mean ± SD of three independent experiments. (J) As in H, except that, where indicated, MBP or MBP-Nvj2ΔTM was added; number of picomole protein added given in parentheses. Mean ± SD of six independent experiments. *, $P < 0.05$, *t* test. 3KS, 3-ketosphinganine; CoA, coenzyme A; MIPC, mannosyl-inositolphosphorylceramide; $M(IP)_2C$, mannosyl-diinositolphosphorylceramide; WT, wild-type.

yeast, the enzyme Aur1p can convert them to inositolphosphorylceramide (IPC), which can subsequently be further glycosylated (Fig. 1 A).

Nonvesicular ceramide transport from the ER to the Golgi complex likely occurs at regions of close contact between these organelles, often called membrane contact sites (MCSs). At these sites, lipid transfer proteins like CERT would have only a short distance to diffuse between membranes. CERT is probably enriched at contact sites, together with other lipid transport proteins (Kumagai et al., 2007; Peretti et al., 2008). In mammalian cells, close contacts between the ER and the Golgi complex, particularly the trans-Golgi, have long been noted

(De Matteis and Rega, 2015). Less is known about ER–Golgi contact in *S. cerevisiae*, though contacts between the ER and cis-Golgi have been observed (Kurokawa et al., 2014). How ER–Golgi contacts are established and regulated is not understood. In mammals, oxysterol-binding protein can tether the ER and Golgi complex (Mesmin et al., 2013), but it is not known whether this protein works in conjunction with other tethers. No ER–Golgi tethers have been identified in *S. cerevisiae*.

In this study, we demonstrate that Nvj2p tethers the ER and medial-Golgi in *S. cerevisiae* and facilitates ceramide transfer between these compartments. Nvj2p resides in the ER. It has a single putative transmembrane (TM) domain and a large cytoplasmic domain that contains a pleckstrin homology (PH) domain and a synaptotagmin-like mitochondrial lipid-binding protein (SMP) domain (Fig. 1 B; Toulmay and Prinz, 2012). SMP domains bind lipids and have recently been found to transfer lipids between membranes (Schauder et al., 2014; AhYoung et al., 2015; Saheki et al., 2016; Yu et al., 2016). We have previously shown that Nvj2p is enriched at a MCS between the nucleus and vacuole, called the nucleus vacuolar junction (NVJ). A tether composed of the ER-resident protein Nvj1p and Vac8p on the vacuole membrane maintain this junction (Pan et al., 2000). In this study, we show that during ER stress or when ceramide levels increase, Nvj2p moves from the NVJ and induces contacts between the ER and medial-Golgi. In addition, we find that Nvj2p-dependent tethering facilitates ceramide transport to the Golgi and prevents the toxic accumulation of ceramides. This is a novel mechanism for preventing toxic lipid accumulation.

Results

A screen for proteins that facilitate ceramide transport from the ER to the Golgi complex

We sought to identify proteins that facilitate nonvesicular ceramide transport from the ER to the Golgi complex in *S. cerevisiae* because it lacks a CERT homologue. A previous study found that a strain lacking three oxysterol-binding protein homologues (*osh234Δ*) has a decreased rate of ceramide transport from the ER to the Golgi complex and suggested that this is because the strain has a defect in vesicular ceramide transport (Fig. 1 A; Kajiwara et al., 2014). This strain consequently has low levels of complex sphingolipids. It is also hypersensitive to aureobasidin A (AbA), which inhibits Aurlp, the enzyme that converts ceramides into the sphingolipid IPC (Fig. 1 A). AbA kills cells because they accumulate toxic amounts of ceramides and have reduced levels of sphingolipids (Cerantola et al., 2009). We suspected that *osh234Δ* cells would become resistant to AbA if a protein that facilitates nonvesicular ceramide transport to the Golgi complex were overexpressed in these cells. Therefore, to identify proteins that may mediate nonvesicular ceramide transport, *osh234Δ* cells were transformed with a high-copy genomic library, and we selected transformants that grew on media with AbA. We identified ∼70 plasmids that allowed the *osh234Δ* mutant to grow on AbA-containing media from ∼8,000 transformants (Table S1). One of these plasmids contained the gene *NVJ2*. Because the plasmid contained several genes in addition to *NVJ2*, we confirmed that *NVJ2* is the complementing gene by generating a high-copy plasmid with only *NVJ2* and found that the plasmid confers AbA resistance to *osh234Δ* cells (unpublished data). Nvj2p has three known domains (Fig. 1 B), and we found that all three are required for Nvj2p to confer resistance to AbA, although the protein lacking the N-terminal TM domain was slightly functional (Fig. S1 A). Interestingly, we found that expression of CERT in *osh234Δ* cells did not confer resistance to AbA (unpublished data), perhaps because CERT cannot bind yeast ceramides that contain long acyl chains.

We suspected that Nvj2p might play a role in nonvesicular ceramide transport for two reasons. First, it contains an SMP domain, which is a lipid-binding domain that can transfer lipids between membranes (Schauder et al., 2014; AhYoung et al., 2015; Saheki et al., 2016; Yu et al., 2016). Second, a large-scale study of protein–lipid interactions suggested that Nvj2p binds ceramide (Gallego et al., 2010).

Nvj2p overexpression facilitates ER-to-Golgi ceramide transport

To determine whether Nvj2p facilitates ceramide transport, we used a well-established assay to measure ER-to-Golgi ceramide transport in cells (Funato and Riezman, 2001). This assay makes use of the fact that ceramide synthesis occurs in the ER, and the enzyme that converts ceramide to IPC (Aur1p) is in the medial-Golgi complex (Dickson and Lester, 1999; Schneiter, 1999; Levine et al., 2000). When cells are incubated with [^{3}H] serine, they produce radiolabeled ceramide, and the conversion of this ceramide to IPC indicates that the ceramide was transferred from the ER to the medial-Golgi (Fig. 1 A). After a 1-h labeling with [^{3}H]serine, the amount of ceramide transport is proportional to the ratio of the radiolabeled IPC to ceramide (Funato and Riezman, 2001; Kajiwara et al., 2014). To calculate this ratio, lipids were separated by TLC (Fig. S1 B), and the ratio was calculated using the ratio of IPC to ceramide (IPC/C); this is the most abundant major complex sphingolipid detected and also used in previous studies (Funato and Riezman, 2001; Kajiwara et al., 2014).

We first confirmed that *osh234Δ* cells have a significant reduction in ceramide transport. In this strain, the IPC/C is 35% that of wild-type cells (Fig. 1 C), as previously reported (Kajiwara et al., 2014). When Nvj2p was overexpressed in *osh234Δ* cells, IPC/C significantly increased to ∼70% of wild-type. We ruled out that this increase was caused by the mislocalization of Aur1-mKate to the ER or increased expression of Aur1p (Fig. S1, C and D). Thus, Nvj2p overexpression increases ER-to-Golgi ceramide transport in *osh234Δ* cells.

Although Nvj2p overexpression increases ceramide transfer, deletion of *NVJ2* (*nvj2Δ*) in *osh234Δ* cells resulted in a nonsignificant decrease in ceramide transport (Fig. 1 C). Consistent with this result, we found that wild-type cells lacking Nvj2p are not hypersensitive to AbA. However, ablation of *NVJ2* in *osh234Δ* renders cells more sensitive to AbA than cells lacking only the Osh proteins (Fig. 1 D), suggesting that elimination of Nvj2p may cause a slight reduction in ER-to-Golgi ceramide transport.

We found that Nvj2p overexpression corrected the ER-to-Golgi ceramide transport defect in a second strain. Cells lacking Arv1p, which plays a role in glycosylphosphatidylinositol anchor synthesis, have reduced vesicular transport of ceramide from the ER to the Golgi complex (Kajiwara et al., 2008). We confirmed this transport defect and found that Nvj2p overexpression partially corrects it (Fig. 1 E). In addition, cells lacking Arv1p are hypersensitive to AbA, like *osh234Δ* cells

(Fig. 1 F). Overexpression of Nvj2p partially restores AbA resistance to cells lacking Arv1p, consistent with a role for Nvj2p in ceramide trafficking.

Because the role of Arv1p and the Osh proteins in vesicular ceramide transport is not understood, we determined whether Nvj2p overexpression was able to correct a ceramide transport defect in cells with a well-characterized defect in vesicular trafficking. Sec18p, the yeast homologue of *N*-ethylmaleimide–sensitive factor, is required for ER-to-Golgi vesicular trafficking. Cells with the conditional *sec18-1* allele have an almost complete block in ER-to-Golgi vesicular trafficking at elevated temperature (Graham and Emr, 1991). It has previously been shown that although ER-to-Golgi vesicular trafficking is blocked in these cells, ER-to-Golgi ceramide transport decreases to 20% that of wild-type cells but is not blocked (Funato and Riezman, 2001; Fig. 1 G), indicating that there is nonvesicular ceramide transport to the Golgi. Overexpression of Nvj2p in *sec18-1* cells partially restored ceramide transport, consistent with the hypothesis that Nvj2p overexpression facilitates nonvesicular ceramide transport. However, Nvj2p may not be the only protein that promotes nonvesicular ceramide transport because it still occurs in *sec18-1* cells lacking Nvj2p (Fig. 1 G). Collectively, these findings suggest that Nvj2p overexpression facilitates ceramide transfer to the Golgi and probably specifically increases nonvesicular ceramide transport.

Nvj2p facilitates nonvesicular ceramide transport in vitro

To more directly determine whether Nvj2p plays a role in nonvesicular ceramide transport, we assessed the ability of Nvj2p to facilitate ceramide transfer in vitro in conditions in which there is no vesicular transport (Funato and Riezman, 2001). To estimate ceramide transport in vitro, we measured the conversion of radiolabeled ceramide (which is generated in the ER) into IPC (which is synthesized in the medial-Golgi). Cell lysates were incubated with the LCB [^{3}H]dihydrosphingosine (DHS), a precursor of ceramide (Fig. 1 A), and the amount of IPC generated in 2 h was determined. We found that lysates from cells overexpressing Nvj2p produced twice as much IPC as wild-type lysates (Fig. 1 H), whereas lysates from cells lacking Nvj2p produced 70% as much IPC as wild type (Fig. 1 I). We ruled out that these differences were caused by differences in the amount of ceramide produced by the lysates (Fig. S1 E). These findings suggest that Nvj2p facilitates nonvesicular transport in vitro.

To confirm that the assay measures nonvesicular ceramide transport, we determined the amount of IPC formation in lysates from *osh234Δ* cells, which have been suggested to have a defect in vesicular but not nonvesicular ceramide transport (Kajiwara et al., 2014). When lysates from wild-type cells and *osh234Δ* cells were labeled with [^{3}H]DHS, we found no difference in the amount of IPC formed (Fig. S1 F). This finding confirmed that *osh234Δ* cells do not have a defect in nonvesicular ceramide transport to the Golgi complex.

We next determined whether the soluble domain of Nvj2p promotes ceramide transfer in vitro. A truncated version of Nvj2p lacking the N-terminal 105 aa of Nvj2p, which includes the putative TM domain, was expressed as a maltose-binding protein (MBP) fusion in yeast and purified. This protein, MBP-Nvj2ΔTM, or MBP alone was added to lysates from wild-type cells or cells lacking Nvj2p. MBP-Nvj2ΔTM increased the amount of ceramide transport, and the increase was proportional to the amount of protein added (Fig. 1 J). This finding may explain why Nvj2ΔTM is slightly functional in cells (Fig. S1 A). The protein may retain enough ability to facilitate ceramide transport that it can partially function in cells when overexpressed. Together, these results support a role for Nvj2p in nonvesicular trafficking of ceramides from the ER to the Golgi.

The SMP domain of Nvj2p is required for nonvesicular ceramide transport

The SMP domain of Nvj2p may directly bind and transport ceramide. To investigate whether lipid binding by the SMP domain is necessary for ceramide transport, we generated mutations in this domain that probably prevent lipid binding. We mutated L340 and I472 of Nvj2p, which correspond to residues in another SMP domain that are predicted to interact with bound lipids and are known to be required for lipid binding (Fig. 2 A; Saheki et al., 2016; Yu et al., 2016). The mutant Nvj2p failed to render *osh234Δ* cells resistant to AbA (Fig. 2 B). It also failed to facilitate ceramide transport to the Golgi in cells (Fig. 2 C) and did not mediate ceramide transport in vitro (Fig. 2 D). We confirmed that the mutant Nvj2p proteins are expressed at the same level as wild-type protein (Fig. S2 A) and have the same localization (not depicted). Together, these findings suggest that the SMP domain of Nvj2p may bind lipids and are consistent with the idea that Nvj2p directly transports ceramide or other lipids.

Nvj2p moves to ER–Golgi MCSs in response to ER stress

How might Nvj2p facilitate ceramide transport to the Golgi complex? We have previously shown that Nvj2-GFP localizes primarily to the NVJ (Toulmay and Prinz, 2012). However, we wondered whether Nvj2p might also be able to localize to ER–Golgi contacts. We reasoned that if Nvj2p localizes to contacts between the ER and medial-Golgi, where Aur1p resides, the two proteins would colocalize when visualized by fluorescence microscopy. To test this, we generated strains that express Nvj2-GFP and Aur1-mKate from their endogenous loci. In wild-type cells, there was little overlap of the signals (Fig. 3 A), and colocalization was observed in only a small percentage of cells (Fig. 3 B). In cells overexpressing Nvj2-GFP, a larger fraction of cells exhibited colocalization of Nvj2-GFP and Aur1-mKate (Fig. 3, A and B).

Because endogenous Nvj2p is highly enriched on the NVJ, we wondered how Nvj2-GFP localization would change in cells lacking the NVJ. In cells lacking Nvj1p (*nvj1Δ*), endogenously expressed Nvj2-GFP colocalizes with Aur1-mKate in the majority of cells (Fig. 3, A and B). This finding suggests that in cells lacking the NVJ, endogenously expressed Nvj2-GFP becomes enriched at ER–Golgi contacts.

Interestingly, we found that Nvj2-GFP is less enriched at the NVJ and more enriched at ER–Golgi contacts when ER function is compromised. Treating cells with 10 mM DTT, which disrupts protein folding in the ER and causes ER stress (Rubio et al., 2011), caused Nvj2-GFP to become enriched at ER–Golgi contacts (Fig. 3, A and B). We ruled out that DTT treatment increased Nvj2p expression (Fig. S2 B). It is likely that DTT treatment affects Nvj2p localization by causing NVJ disassemble (Fig. S2 C), releasing Nvj2p from the NVJ. Nvj2-GFP enrichment at ER–Golgi contacts was also caused by inhibition of vesicular trafficking from the ER. When *sec18-1* cells were shifted to nonpermissive temperature for 1 h, most Nvj2-GFP did not remain at the NVJ (Fig. 3 C). This finding also

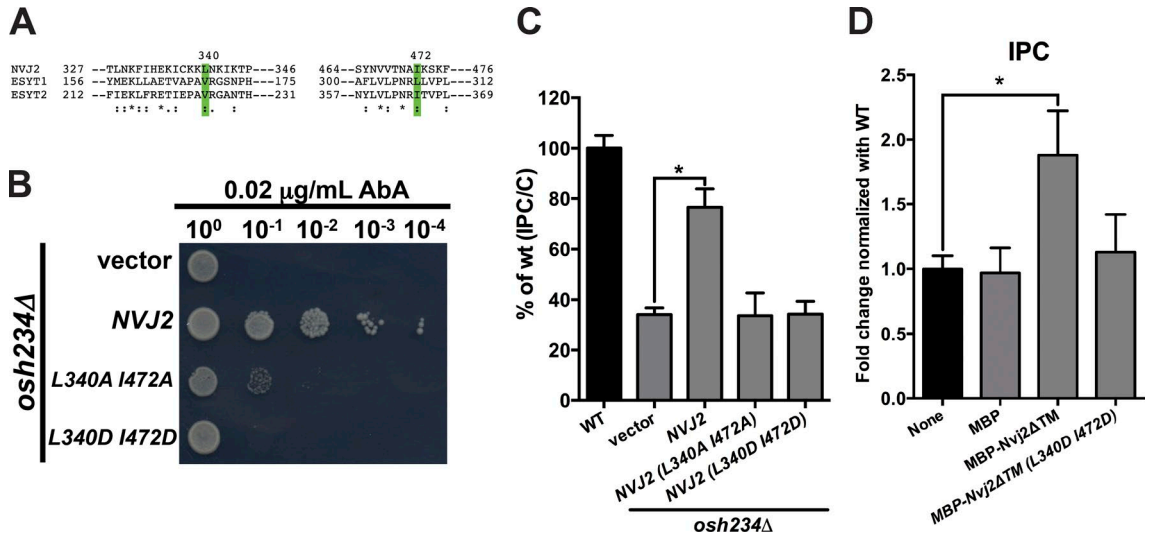

Figure 2. **The SMP domain of Nvj2 is required for nonvesicular ceramide transport.** (A) Alignment of a portion of the Nvj2p SMP domain with those from human E-Syts using Clustal Omega. Residues L340 and I472 in Nvj2p are equivalent to V159 and L298 of the SMP domain from E-Syt1 (green). These residues in E-Syt1 are necessary for lipid binding and may contact bound lipids. (B) Serial dilutions of *osh234Δ* cells with the indicated plasmids on plates containing 0.02 µg/ml AbA. (C) Cells were labeled with [^{3}H]serine as in Fig. 1 C. Mean ± SD of three independent experiments. (D) Lysates from wild-type cells and 500 pmol of the indicated proteins were labeled with [^{3}H]DHS for 2 h at 25°C, and the relative amount of radiolabeled IPC formed was determined. Mean ± SD of six independent experiments. *, $P < 0.05$, *t* test.

suggests that Nvj2-GFP does not traffic to the Golgi complex but instead diffuses in the ER from the NVJ to ER–Golgi MCSs because Sec18p is required for vesicular transport from the ER.

We suspected that the PH domain of Nvj2p might bind the Golgi complex and help localize the protein to ER–Golgi contacts. Indeed, we found that a truncated version of Nvj2p containing only the TM and PH domains colocalizes with Aur1-mKate (Fig. S2 D), suggesting that the PH domain interacts with the Golgi. Interestingly, Nvj2p lacking only the PH domain did not remain at the NVJ but was all over the ER (Fig. S2 D), indicating that the PH domain is also necessary for Nvj2p to bind the vacuole. We also investigated the ability of Nvj2p to tether liposomes in vitro. To do this, we purified a version of Nvj2p in which the N-terminal 40 residues of the protein, which contain the TM domain, were replaced with MBP and a His tag. The resulting protein, MBP-His_{x9}-Nvj2, was bound to liposomes that included a nickel-containing lipid and were filled with sucrose, allowing them to be pelleted at low speed. These liposomes were mixed with a second set of liposomes that did not contain sucrose and would not pellet at low speed unless Nvj2p tethered them to the sucrose-filled liposomes (Fig. S2 E). Using this assay, we found that Nvj2p can tether liposomes and that tethering was improved when phosphatidylinositol phosphates (PIPs) or phosphatidic acid (PA) were present in the liposomes (Fig. 3 D). Thus, the cytoplasmic domain of Nvj2p has affinity for charged liposomes, but there was little PIP specificity. These findings indicate that Nvj2p can directly tether membranes. The PH domain of Nvj2p is required for Golgi membrane binding but does not seem to have much specificity for individual PIPs, consistent with an earlier study (Yu et al., 2004). Thus, it remains unclear whether the PH domain allows Nvj2p to bind Golgi membranes.

Collectively, these findings suggest that Nvj2-GFP resides largely at the NVJ in unstressed cells, but when this fusion is overexpressed or during ER stress, Nvj2-GFP diffuses in the ER and becomes enriched at ER–Golgi contacts. The PH domain of Nvj2p is required for it to bind the Golgi membrane.

Nvj2p increases ER–Golgi tethering during ER stress

Because Nvj2p becomes enriched at ER–Golgi contacts during ER stress, we wondered whether ER–Golgi contacts increase during ER stress and, if so, whether Nvj2p is necessary for this increase. We first used fluorescence microscopy to assess contacts between the ER and medial-Golgi. We visualized cells expressing the ER marker Sec61-GFP and the medial-Golgi marker Aur1-mKate and quantitated how often Aur1-mKate puncta colocalized with the ER ("on"), were next to the ER ("associated"), or were not associated with the ER ("away"). In unperturbed wild-type cells, most Aur1-mKate puncta were away from the ER (Fig. 4, A and B). Treating cells with DTT caused ∼75% of Golgi vesicles containing Aur1-mKate to colocalize with or be closely associated with the ER (Fig. 4, A and B), suggesting that ER–Golgi contacts increase during ER stress. Of the Golgi vesicles that associate with the ER during stress, ∼60% contact the cortical ER and the rest contact perinuclear ER (Fig. S2 F). Remarkably, there was little increase in ER–Golgi contact in *nvj2Δ* cells when they were treated with DTT (Fig. 4 B). This finding suggests that most of the increase in association of the ER and Golgi during ER stress is Nvj2p dependent.

Consistent with Nvj2p driving ER–Golgi tethering, we found that Nvj2p overexpression, which causes a fraction of Nvj2p to localize to ER–Golgi contacts (Fig. 3 A), resulted in an increased association of the Aur1-mKate–containing Golgi compartments with the ER (Fig. 4, C and D). Collectively, these results suggest that Nvj2p induces contacts between the ER and Golgi complex during ER stress.

We confirmed these results using EM. To identify Golgi compartments containing Aur1p, we fused ascorbate peroxidase (APEX2) (Martell et al., 2012; Lam et al., 2015) to the C terminus of Aur1-GFP. We confirmed that the resulting protein, Aur1-GFP-APEX2, remains in the Golgi using fluorescence microscopy (unpublished data). APEX2 produces a precipitate that gives EM contrast after treatment with OsO_4 (Fig. S3 A),

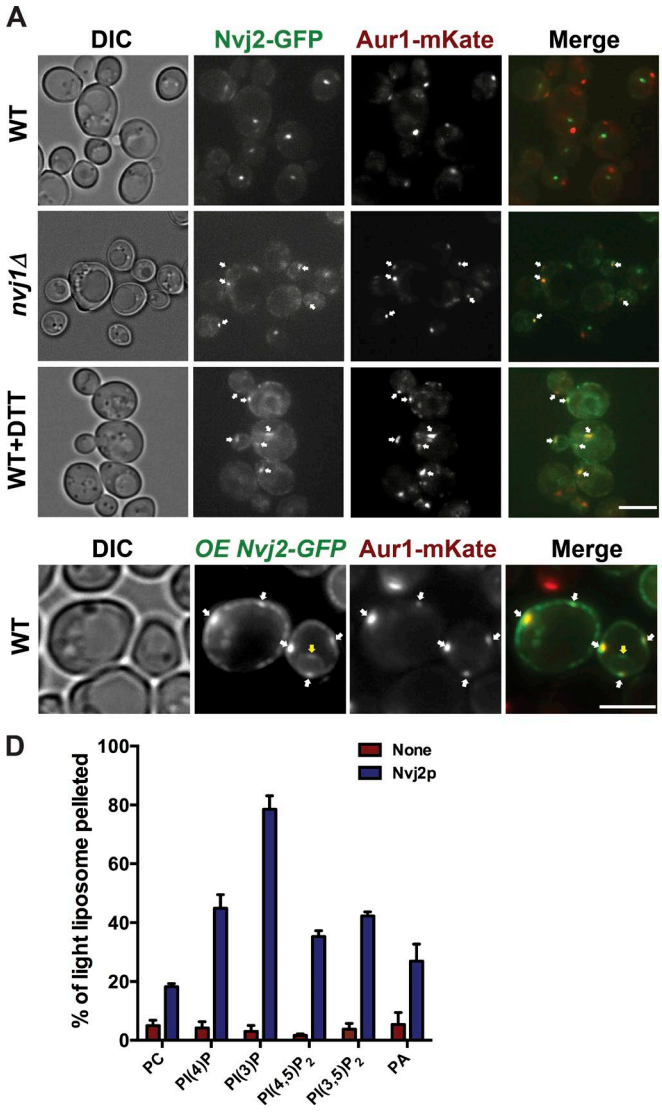

Figure 3. **Nvj2-GFP and Aur1-mKate colocalize during ER stress.** (A) Cells expressing Nvj2-GFP from the chromosome or from a plasmid (OE Nvj2-GFP) and endogenously tagged Aur1-mKate were grown at 30°C and visualized live. Where indicated, cells were treated with 10 mM DTT for 4 h before visualization. White arrows indicate areas of Aur1-mKate and Nvj2-GFP colocalization. Yellow arrows indicate the NVJ. Bars, 5 µm. (B and C) Percent of cells in which Nvj2-GFP and Aur1-mKate colocalized. Mean ± SD of three independent experiments. n = 400 (B) or 200 (C) cells. (D) Tethering of liposomes by Nvj2p. MBP-His_{x9}-Nvj2p (100 pmol) was incubated at 30°C with liposomes that do not contain sucrose (light) and sucrose-filled liposomes (heavy) that include 5% of a nickel-containing lipid. The light liposomes included various PIPs or other lipids. At 16,000 *g*, the heavy liposomes pellet, but the light liposomes will only pellet if they are tethered to the heavy liposomes. *, $P < 0.05$, *t* test. The amount of these lipids in the liposomes was either 10 mol% [PC, PA, PI(3)P, and PI(4)P)] or 5 mol% [$PI(3,5)P_2$ and $PI(4,5)P_2$]. Mean ± SD of three independent experiments. DIC, differential interference contrast; PI(3)P, phosphatidylinositol 3-phosphate; PI(4)P, phosphatidylinositol 4-phosphate; $PI(3,5)P_2$, phosphatidylinositol 3,5-bisphosphate; $PI(4,5)P_2$, phosphatidylinositol 4,5-bisphosphate; WT, wild-type.

which allowed us to identify compartments containing Aur1-GFP-APEX2 (i.e., the medial-Golgi). We confirmed that no precipitate was visible in cells not express the fusion protein (Fig. S3 B). In wild-type cells with Aur1-GFP-APEX2, the ER was rarely associated with the medial-Golgi and only ∼15% of medial-Golgi vesicles had ER within 20 nm of them (Fig. 5, A and E). However, when cells were treated with DTT or when Nvj2p was overexpressed there was a dramatic increase in ER association with the medial-Golgi (Fig. 5, B, C, and E). No increase in ER–Golgi contact was seen when *nvj2Δ* cells were treated with DTT (Fig. 5, D and E), consistent the results from fluorescence microscopy (Fig. 4) and with the hypothesis that increased tethering during ER stress requires Nvj2p.

Because the treatment required to visualize APEX2 reduced image quality, we also visualized wild-type cells expressing Aur1-GFP without APEX2. In wild-type cells that were not treated with DTT, the ER was not usually associated with vesicles that were probably the Golgi (Fig. 5 F). The ER was frequently associated with Golgi-like vesicles when wild-type cells were treated with DTT (Fig. 5 G) but not when *nvj2Δ* cells were treated with DTT (Fig. 5 H). Overexpression of Nvj2p in wild-type cells increased ER association with vesicles that are probably the medial-Golgi (Fig. 5 I and Fig. S3 C). Collectively, our findings indicate that ER–Golgi contacts increase dramatically after DTT treatment, which induces ER stress, and this increase requires Nvj2p.

An artificial ER–Golgi tether can partially substitute for Nvj2p

Because Nvj2p can tether the ER and medial-Golgi, we wondered whether increased tethering is sufficient to increase ceramide transport from the ER to the Golgi. To test this, we generated an artificial ER–Golgi tether and determined whether it would increase ER-to-Golgi ceramide transport. We fused the TM domain of the Golgi-resident protein Svp26p to GFP and the tail-anchored TM domain from Ubc6p (Fig. 6 A). This region of Ubc6p has been previously used in an ER–mitochondria artificial tether (Kornmann et al., 2009). We named the Svp26-GFP-Ubc6 tether EGT. EGT was largely in punctate structures that colocalized with the cis-Golgi and medial-Golgi (Fig. S4 A).

EGT partially rescued the ceramide transport defect in *osh234Δ* cells; it rendered them more resistant to AbA (Fig. 6 B) and increased conversion of ceramide to IPC (Fig. 6 C). EGT did not alter the location of Aur1-mKate (Fig. S4 B). It also did not increase ceramide transport in wild-type cells but did partially restore ceramide transport in *sec18-1* cells (Fig. 6 D),

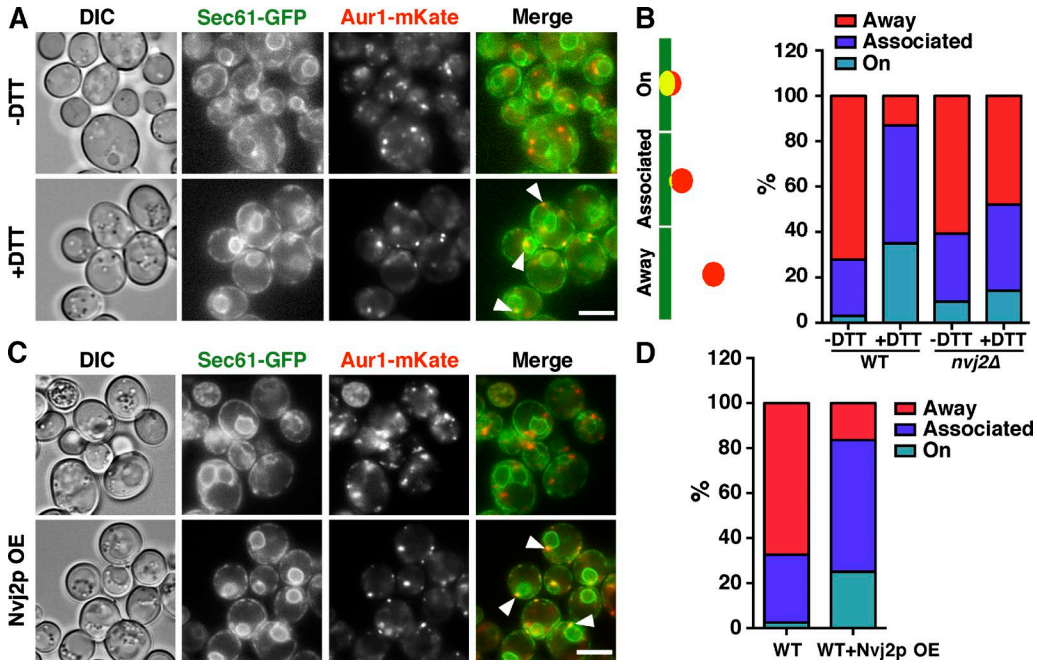

Figure 4. **Nvj2p forms and increases ER–Golgi contacts during ER stress.** (A) Cells expressing endogenously tagged Sec61-GFP (ER; green) and Aur1-mKate (medial-Golgi; red) were grown in media with or without DTT for 4 h. White arrowheads indicate areas of Aur1-mKate and Sec61-GFP colocalization. (B) Quantification of experiments in A. Aur1-mKate puncta were classified as "on" the ER (colocalize with ER), "associated" with (next to) the ER, or "away" from the ER. Three independent experiments; n = 400 cells. (C) As in A, except that cells either did or did not overexpress (OE) Nvj2p. (D) Quantification of experiment in C as in B. Three independent experiments; n = 350 cells. Bars, 5 µm. DIC, differential interference contrast; WT, wild-type.

suggesting that it specifically enhances nonvesicular ceramide transport to the Golgi complex. To more directly visualize this, we used the in vitro ceramide transport assay to compare the amount of ceramide transport in lysates from wild-type cells with lysates from cells expressing EGT. There was about two-fold more IPC formed in lysates from cells expressing EGT (Fig. 6 E), consistent with the idea that EGT enhances nonvesicular ceramide transport. We ruled out that lysates from cells expressing EGT produced a different amount of ceramide than lysates made from cells not expressing EGT (Fig. S4 C). Interestingly, EGT was not able to restore ceramide transfer in *sec18-1* lacking cells Nvj2p (*sec18-1 nvj2Δ*) as well it could in *sec18-1* cells (Fig. 6 D). Thus, EGT may not be able to completely replace Nvj2p. This may be because Nvj2p directly facilitates ceramide transport in addition to functioning as a tether. This finding also indicates that proteins in addition to Nvj2p facilitate nonvesicular ceramide transport, consistent with the result in Fig. 1 I. Collectively, these findings support the conclusion that Nvj2p can promote nonvesicular ceramide transport from the ER to the Golgi complex by tethering them and suggest that Nvj2p may also directly transport ceramide.

Only ER-Golgi contact-localized Nvj2p promotes ceramide transport to the Golgi complex. Our findings suggest that Nvj2p facilitates ER–Golgi tethering and nonvesicular ceramide transfer from the ER to the Golgi complex. We determined whether Nvj2p must be localized to ER–Golgi contacts to promote ceramide transport to the Golgi complex or whether Nvj2p at the NVJ indirectly promotes ceramide transfer. We first determined whether the NVJ is necessary for overexpressed Nvj2p to complement the AbA sensitivity of *osh234Δ* cells. We found that Nvj2p complements *osh234Δ* cells that also lack Nvj1p (and hence the NVJ), suggesting that Nvj2p localization to the NVJ is not necessary for it to facilitate ceramide transport to the Golgi (Fig. 7 A).

We next asked whether Nvj2p facilitates ceramide transport to the Golgi complex when it restricted to the perinuclear ER (including the NVJ) and cannot reach portions of the ER that form ER–Golgi junctions. It has previously been found that the N-terminal portion of Nvj1p (aa 1–120) resides only in the outer nuclear membrane and not the remainder of the ER (Kvam and Goldfarb, 2006). We replaced the TM domain of Nvj2p with the N-terminal 120 residues of Nvj1 (Nvj1(1–120)-Nvj2ΔTM; Fig. 7 B). We found that Nvj1(1–120)-Nvj2ΔTM was only in the perinuclear ER but not cortical ER (Fig. 7 C), even during ER stress (Fig. S5 A), and was not able to complement the AbA sensitivity of *osh234Δ* cells (Fig. 7 D). These results suggest that when Nvj2p is not at ER–Golgi contacts, it cannot facilitate ceramide transport to the Golgi complex. To rule out that Nvj1(1–120)-Nvj2ΔTM failed to complement *osh234Δ* cells because the TM portion of Nvj2p has a function in addition to anchoring the protein in the ER, we replaced the TM domain of Nvj2p with Sec63p, an ER-resident protein that has its C terminus in the cytoplasm. The resulting fusion protein, Sec63-Nvj2ΔTM, localized to the ER and was enriched at puncta that are ER–Golgi junctions (Fig. 7 E, left panels). It was able to complement *osh234Δ nvj1Δ* cells (Fig. 7 E, right panels). We also found that Sec63-Nvj2ΔTM, but not Nvj1(1–120)-Nvj2ΔTM, restored ceramide transport in *osh234Δ* cells (Fig. 7 F). Collectively, these results suggest that Nvj2p must be enriched at ER–Golgi contacts to facilitate ceramide transport from the ER to the Golgi complex.

Nvj2p prevents the toxic accumulation of ceramides

We speculated that Nvj2p increases ER–Golgi tethering during ER stress to promote ceramide transfer out of the ER and prevent the toxic accumulation of ceramide. To test this, we investigated whether Nvj2p allows cells to tolerate elevated ceramide

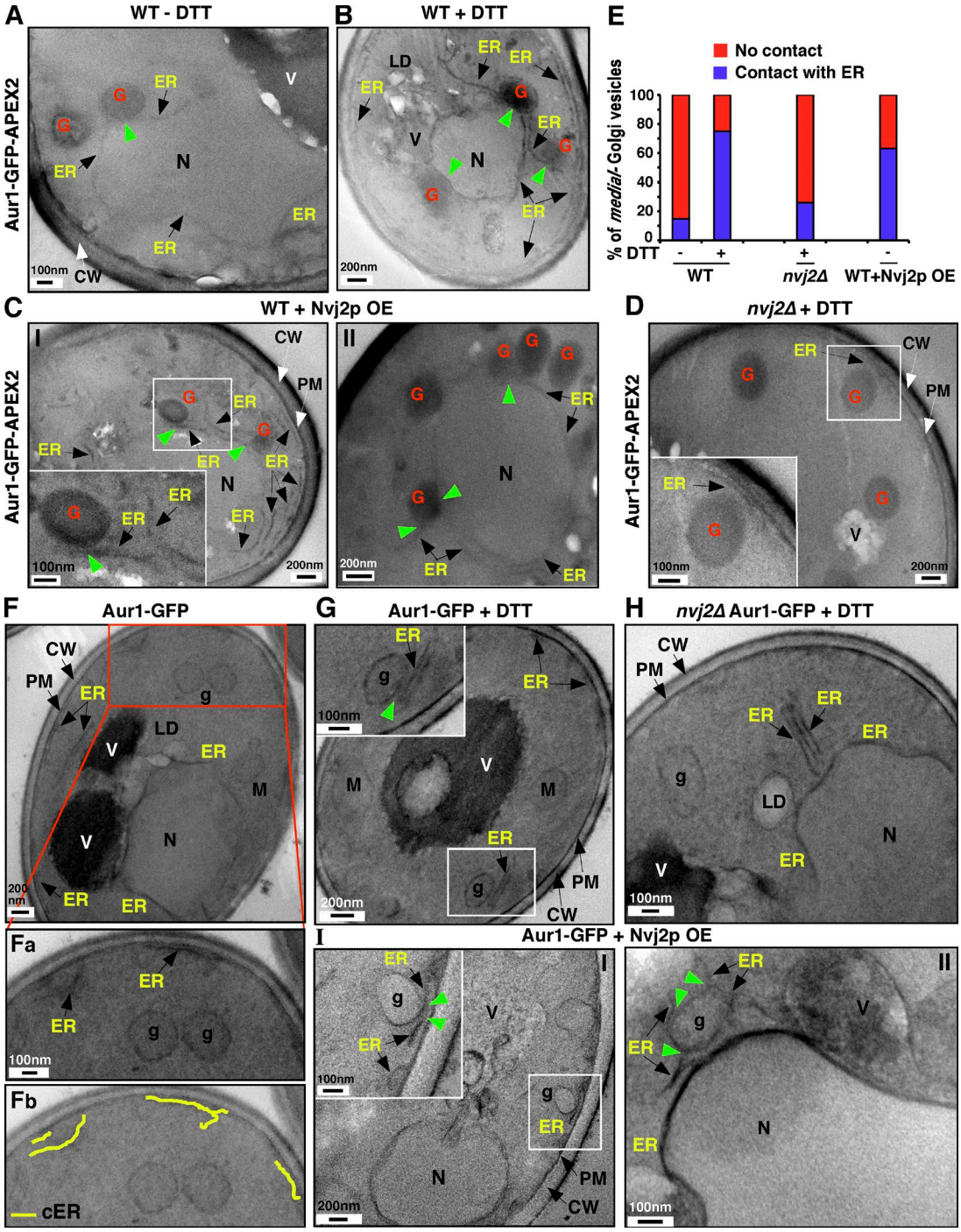

Figure 5. **Using EM to show that Nvj2p forms and increases ER–Golgi contacts during ER stress.** (A–D) EM of indicated strains expressing the medial-Golgi maker Aur1-GFP-APEX2, which forms a black precipitate. Where indicated, cells were grown with 10 mM DTT for 4 h before visualization. Boxed regions shown in higher magnification in insets. Green arrowheads show contact between ER and medial-Golgi compartment. Two examples (I and II) are shown in C. (E) Quantification of experiments in A–D. Percent of APEX2-positive vesicles (i.e., medial-Golgi) within ~20 nm of the ER. *n* = 40 cells per strain and condition. (F–I) EM of chemically fixed cells. Boxed regions shown in higher magnification in insets. Trace of cortical ER (cER) in Fa is shown in Fb in yellow. Green arrowheads show contact between the ER and Golgi-like vesicles. CW, cell wall; g, Golgi-like; G, medial-Golgi; LD, lipid droplet; N, nucleus; OE, overexpressed; PM, plasma membrane; V, vacuole; WT, wild-type.

synthesis and prevents ceramide accumulation. It has been found that overexpression of the ceramide synthase Lag1p increases ceramide levels and decreases growth rate (Kim et al., 2010). We introduced into wild-type cells a plasmid expressing Lag1p under the galactose-inducible *GAL1* promoter. When the cells were transferred to a galactose-containing medium, their growth rate significantly decreased, and ceramide levels increased (Fig. 8, A and B). These defects were partially corrected by Nvj2p overexpression (Fig. 8, A and B). We confirmed that all of the strains tested grew at similar rates in a medium with glucose, in which the *GAL1* promoter is not active (Fig. S5 B). These findings indicate that Nvj2p overexpression

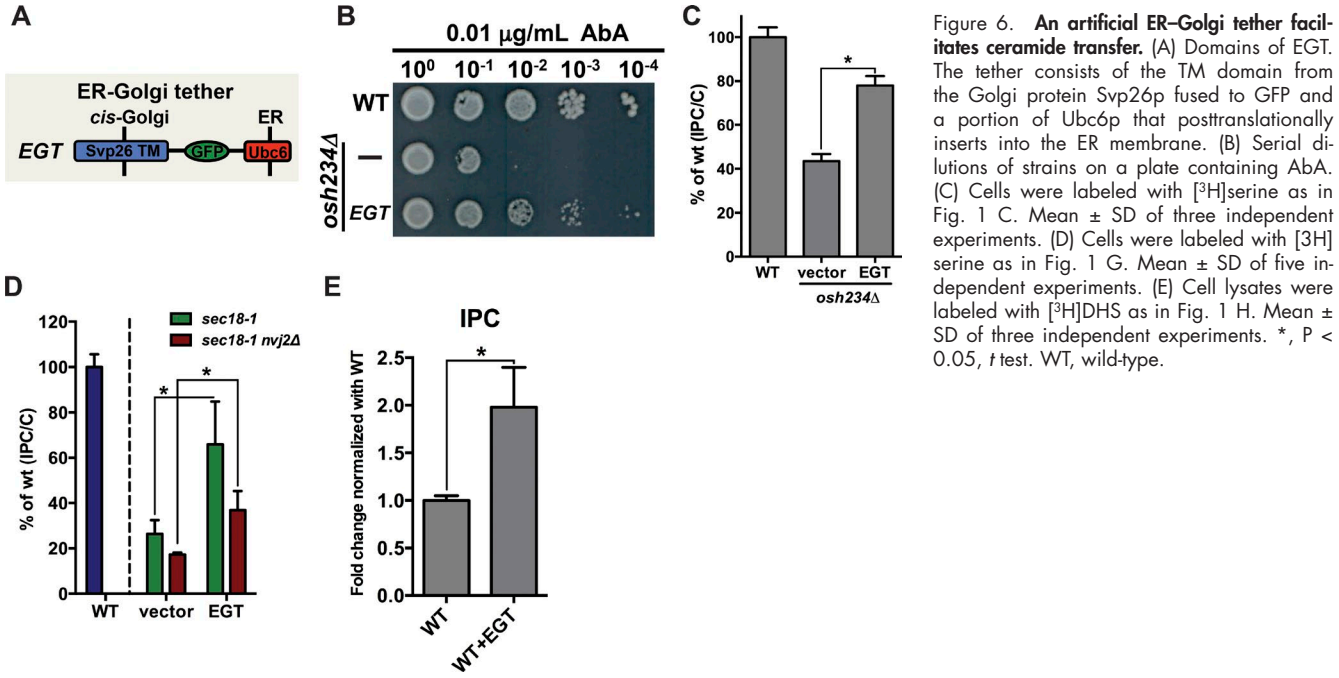

Figure 6. **An artificial ER–Golgi tether facilitates ceramide transfer.** (A) Domains of EGT. The tether consists of the TM domain from the Golgi protein Svp26p fused to GFP and a portion of Ubc6p that posttranslationally inserts into the ER membrane. (B) Serial dilutions of strains on a plate containing AbA. (C) Cells were labeled with [^{3}H]serine as in Fig. 1 C. Mean ± SD of three independent experiments. (D) Cells were labeled with [3H] serine as in Fig. 1 G. Mean ± SD of five independent experiments. (E) Cell lysates were labeled with [^{3}H]DHS as in Fig. 1 H. Mean ± SD of three independent experiments. *, $P < 0.05$, *t* test. WT, wild-type.

reduces ceramide levels and prevents cells from accumulating toxic amounts of ceramide, probably by facilitating ceramide transfer out of the ER.

To confirm that Nvj2p overexpression reduces ceramide levels, we used another strain that overproduces ceramide. Orm1p and Orm2p are conserved regulators of the rate-limiting step in ceramide biosynthesis, the formation of 3-ketosphinganine by serine palmitoyltransferase (Breslow et al., 2010; Han et al., 2010; Fig. 1 A). Cells lacking Orm1p and Orm2p (*orm1Δ orm2Δ*) have increased levels of LCBs and ceramides, which cause constitutive ER stress, impair vesicular transport, and slow growth (Breslow et al., 2010; Han et al., 2010; Shimobayashi et al., 2013). We investigated whether overexpression of Nvj2p corrected these defects and lack of Nvj2p exacerbated them.

We first confirmed that the ER stress and other defects in *orm1Δ orm2Δ* cells are primarily caused by the accumulation of toxic levels of ceramide. Cells lacking Orm1p and Orm2p are hypersensitive to tunicamycin (Fig. S5 C), an inhibitor of *N*-linked glycosylation (Hjelmqvist et al., 2002; Han et al., 2010) that induces ER stress. This hypersensitivity can be partially reversed by deletion of *LAG1* or *LAC1*, genes that encode the two ceramide synthases in yeast (Fig. 1 A). It has previously been shown that cells lacking either of these synthases have reduced levels of ceramides (Schorling et al., 2001; Rego et al., 2012; Martínez-Montañés and Schneiter, 2016). In contrast, cells lacking Orm1p, Orm2p, and Lcb4p, which phosphorylates sphingosine and other LCBs, remain hypersensitive to tunicamycin (Fig. S5 C). Collectively, these findings suggest that the hypersensitivity of *orm1Δ orm2Δ* cells to tunicamycin is caused by the accumulation of ceramide in these cells.

We found that overexpression of Nvj2p in *orm1Δ orm2Δ* cells rendered them resistant to tunicamycin (Fig. 8 C), indicating that Nvj2p overexpression reduces ER stress in *orm1Δ orm2Δ* cells. To verify this, we used a reporter of ER stress, UPRE-lacZ, in which LacZ expression is controlled by the unfolded protein response promoter element (UPRE). We confirmed that treating cells with DTT induces ER stress (Fig. 8 D). In cells lacking Orm1p and Orm2p, ER stress is constitutive without DTT treatment and is further induced by DTT (Fig. 8 D; Han et al., 2010; Liu et al., 2012). Remarkably, overexpression of Nvj2p or Orm1p in *orm1Δ orm2Δ* cells reduces ER stress in these cells to levels that are similar to wild-type cells (Fig. 8 D). We found that Nvj2p reduces ER stress in *orm1Δ orm2Δ* cells because it decreases ceramide amounts to levels similar to those of wild-type cells (Fig. 8 E). The overexpression of Nvj2p, but not Orm1p, increased the IPC produced in 1 h (Fig. 8 F), as would be expected if Nvj2p increases the amount of ceramide transferred to the Golgi complex where the ceramide is converted to IPC. Consistent with a role for Nvj2p in ER-to-Golgi ceramide transfer, we found Nvj2-GFP is enriched at ER–Golgi contacts in *orm1Δ orm2Δ* cells (Fig. 8 G). To rule out the possibility that Nvj2p negatively regulates serine palmitoyltransferase, as the Orm proteins do, we measured levels of DHS in *orm1Δ orm2Δ* cells overexpressing Nvj2p. No significant difference of DHS levels was found in *orm1Δ orm2Δ* cells whether or not they overexpressed Nvj2p (Fig. S5 D), suggesting that Nvj2p is not a negative regulator of serine palmitoyltransferase.

Although overexpression of Nvj2p in *orm1Δ orm2Δ* cells reduces ER stress, elimination of Nvj2p increases ER stress; cells lacking Orm1p, Orm2p, and Nvj2p (*orm1Δ orm2Δ nvj2Δ*) are more sensitive to tunicamycin than *orm1Δ orm2Δ* cells (Fig. 8 H). This increased sensitivity is probably because *orm1Δ orm2Δ nvj2Δ* cells accumulate significantly more ceramide during ER stress than *orm1Δ orm2Δ* cells (Fig. 8 I).

To obtain further evidence that Nvj2p overexpression protects cells from toxic ceramide accumulation during stress, we determined whether Nvj2p could protect cells in growth conditions that cause them to accumulate toxic amounts of ceramide. It has been suggested that yeast undergo an apoptosis-like programmed cell death in response to treatment with acetic acid, which leads to the accumulation of high levels of ceramide (Rego et al., 2012). This study showed that cells lacking Lag1p, one of the two ceramide synthases in yeast (Fig. 1 A), have lower levels of ceramide than wild-type cells and are better able to survive

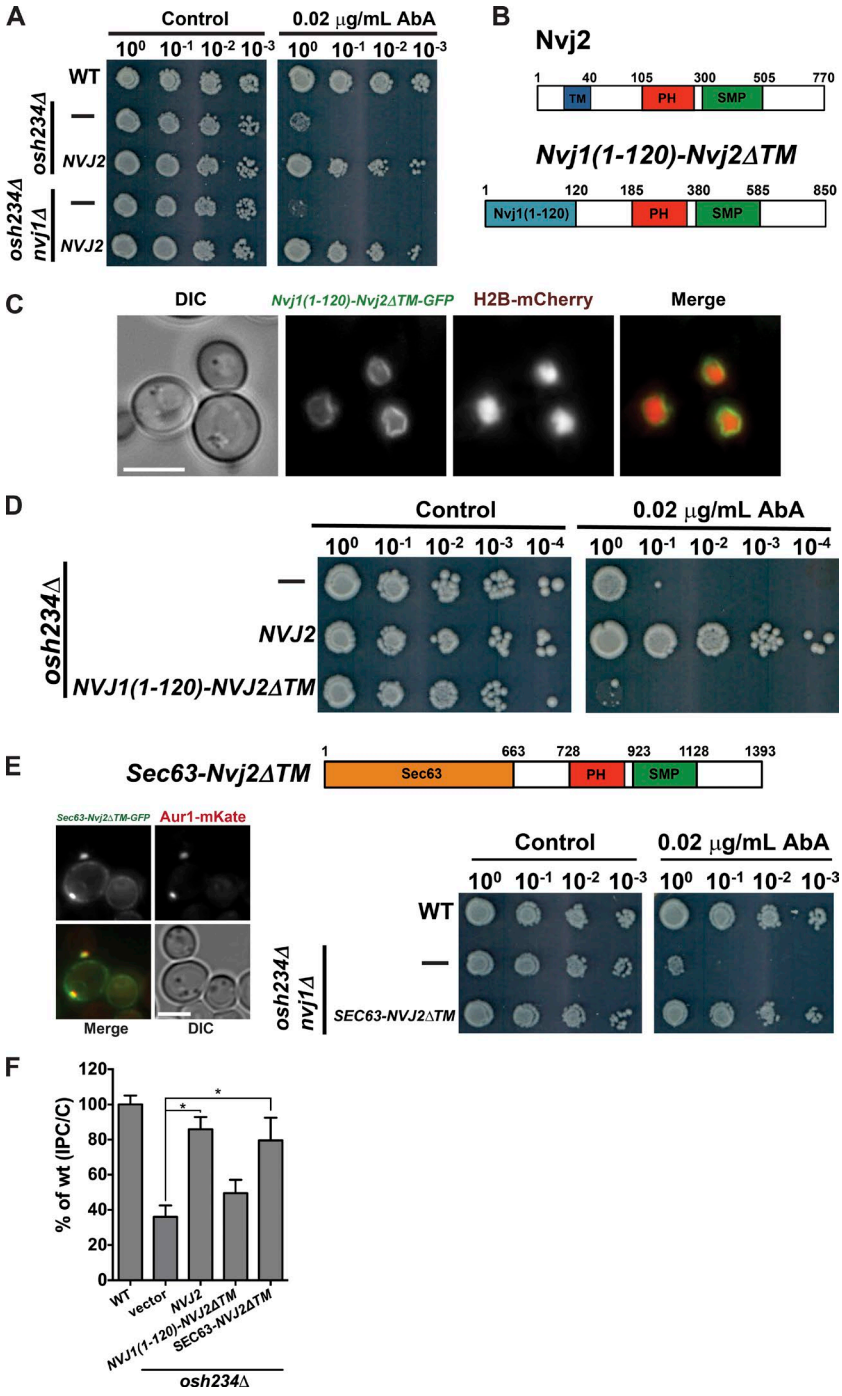

Figure 7. **Nvj2p promotes ceramide transport to the Golgi at ER–Golgi contacts.** (A and D) Serial dilutions of strains grown with or without AbA. (B) Domains of Nvj2p and *Nvj1(1–120)-Nvj2ΔTM*. Numbers indicate amino acids. (C) Cell expressing *Nvj1(1–120)-Nvj2ΔTM-GFP* (green) and histone H2B-mCherry (red). (E) Diagram of *Sec63-Nvj2ΔTM* chimera protein; numbers indicate amino acids (top panel). Cells expressing *Sec63-Nvj2ΔTM*-GFP (green) and Aur1-mKate (red; left panel). Serial dilutions of strains grown with or without AbA (right panel). (F) Cells were labeled with [^{3}H]serine as in Fig. 1 C. Mean ± SD of three independent experiments. Bars, 5 µm. *, $P < 0.05$, *t* test. DIC, differential interference contrast; WT, wild-type.

from treatment with acetic acid. We confirmed that cells lacking Lag1p are better able to survive acetic acid treatment than wild types (Fig. 8 J). Interestingly, overexpression of Nvj2p also protects wild-type cells from acetic acid exposure (Fig. 8 J), consistent with the model that Nvj2p overexpression helps cell survive from the toxic accumulation of ceramides. Cells lacking Lag1p and overexpressing Nvj2p were the most resistant to acetic acid treatment (Fig. 8 J). Collectively, our findings indicate that Nvj2p can prevent ceramide accumulation and alleviate ceramide toxicity caused by ER stress or other conditions that increase ceramide levels.

Two pathways prevent ceramide toxicity during stress

It has previously been found that ceramide can be converted to acylceramides (Voynova et al., 2012), which may be a method for preventing the accumulation of excess ceramide. Lro1p and Dga1p, acyltransferases that primarily produce triacylglycerol, generate acylceramides. If one of the major functions of Nvj2p is to prevent ceramide accumulation during stress, we speculated that cells lacking Nvj2p, Lro1p, and Dga1p (*dga1Δ lro1Δ nvj2Δ*) might have very high levels of ceramide during ER stress. Consistent with this, we found that *dga1Δ lro1Δ nvj2Δ* cells have about eightfold more ceramide then wild-type cells

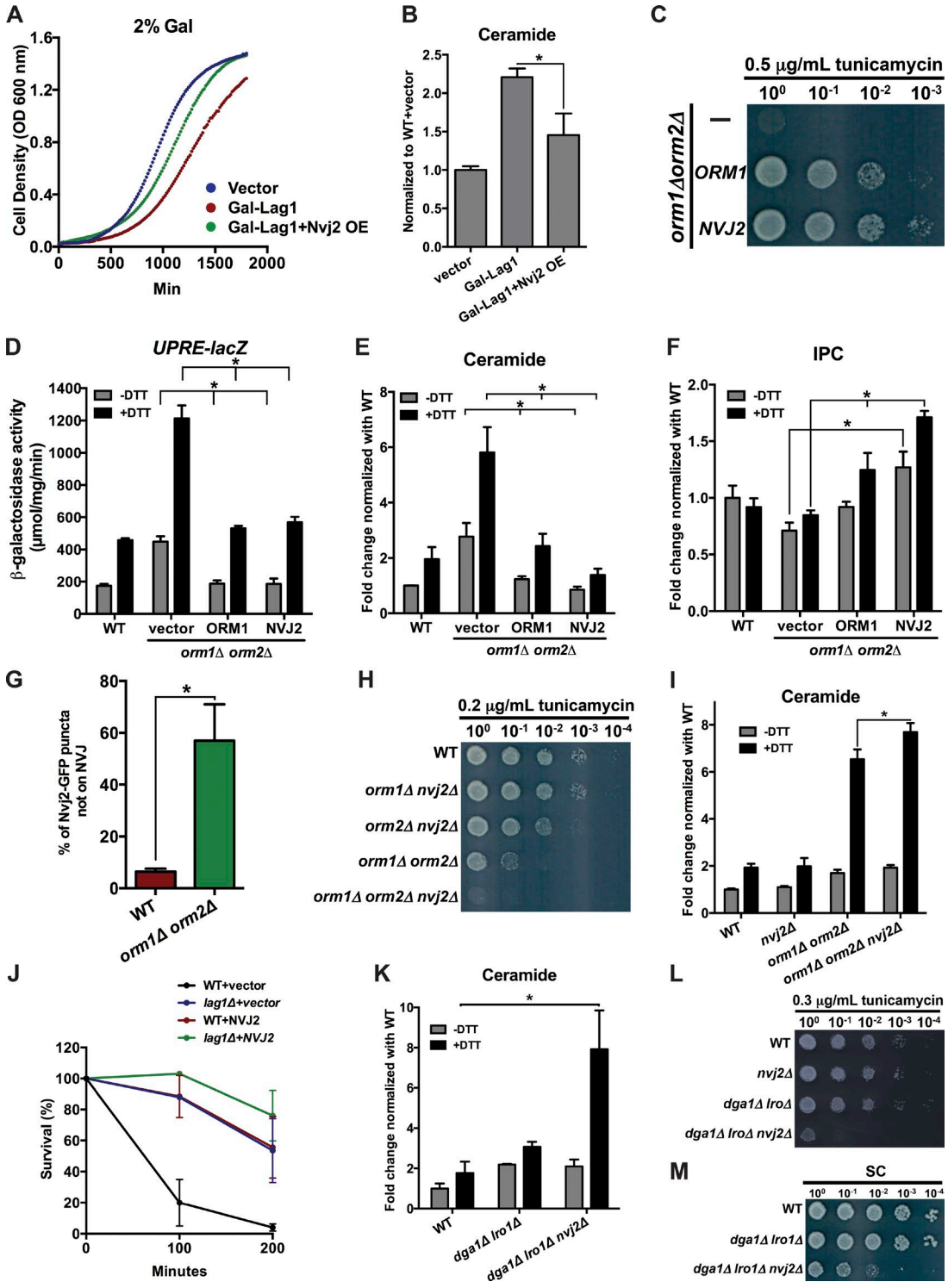

Figure 8. **Nvj2p alleviates ceramide toxicity.** (A) Growth of wild-type (WT) cells with indicated plasmids after addition of galactose to the medium. (B) Relative amount of ceramide in the strains in A 8 h after addition of galactose. Mean ± SD of three independent experiments. (C, H, L, and M) Serial dilutions of strains grown with indicated amount of tunicamycin. (D) β-Galactosidase activity of strains containing the ER stress reporter *UPRE-lacZ* after growth for 1 h in media with or without DTT. Mean ± SD of six independent experiments. (E, I, and K) Cells were grown in media with or without DTT for 4 h, labeled for 4 h with [^{3}H]palmitic acid, and the relative amount of radiolabeled ceramide determined. Mean ± SD of six independent experiments, (F) Cells were grown in media with or without DTT for 4 h, labeled for 1 h with [^{3}H]serine, and the relative amount of radiolabeled IPC determined. Mean ± SD of three independent experiments. (G) Percent of cells in which Nvj2-GFP and Aur1-mKate colocalized. Mean ± SD of three independent experiments. n = 400 cells. (J) Survival of indicated stains exposed to 180 mM acetic acid for up to 200 min. Cell viability was determined by standard dilution plate counts and expressed as a percentage of colony-forming units on YPD plates. Mean ± SD of three independent experiments. *, $P < 0.05$, t test.

when they are treated with DTT. The roles of Nvj2p and acylceramide production by Dga1p and Lro1p in preventing ceramide accumulation during stress seem to be redundant because cells lacking only Nvj2p do not have elevated ceramide (Fig. 8 I), and a strain lacking Dga1p and Lro1p had only about twofold higher ceramide levels than wild-type cells (Fig. 8 K; Voynova et al., 2012). We found that *dga1Δ lro1Δ nvj2Δ* cells are hypersensitive to tunicamycin (Fig. 8 L), suggesting that the elevated ceramide in this strain during ER stress is toxic. These findings suggest that yeast has two pathways that normally prevent the toxic accumulation of ceramides during ER stress. Interestingly, cells lacking Lro1p, Dga1p, and Nvj2p grow poorly even in the absence of ER stress (Fig. 8 M), suggesting that these proteins may also prevent the accumulation of DAG or other toxic lipid intermediates in unstressed cells. It may be that Nvj2p can transport DAG (or other lipids).

Nvj2p homologues are functional in yeast

Nvj2p has homologues in higher eukaryotes. To determine whether they might have functions similar to Nvj2p, we expressed those from *Arabidopsis thaliana* (AT1G73200) and humans (HT008, also known as TEX2) in yeast. AT1G73200 functioned as well as Nvj2p in *osh234Δ* cells, whereas HT008 was partially functional (Fig. 9 A). AT1G73200 was also able to facilitate ceramide transport in yeast (Fig. 9 B). We used a second genetic method to assess whether Nvj2p homologues can functionally replace Nvj2p. Cells lacking Nvj2p are resistant to fenpropimorph (Toulmay and Prinz, 2012), which inhibits sterol biosynthesis. We found that both AT1G73200 and HT008 restored fenpropimorph sensitivity to cells lacking Nvj2p, though HT008 was only partially functional (Fig. 9 C). These findings suggest that Nvj2p and its homologues in higher eukaryotes may have similar roles in ceramide transport and contact site formation. The difference in the ability of HT008 and AT1G73200 to replace Nvj2p in yeast may reflect that fact that yeast ceramides and other sphingolipids are more similar to those of plants than those of mammals (Megyeri et al., 2016; Michaelson et al., 2016).

Discussion

In this study, we show that contacts between the ER and medial-Golgi complex increase dramatically during ER stress and when ceramide levels increase. Formation of these contacts requires Nvj2p, which localizes to contact sites and probably directly tethers the ER and Golgi membranes, though it may work in concert with other proteins. Increased contact between the ER and medial-Golgi facilitates ceramide transfer from the ER, where ceramides are synthesized, to the Golgi, where Aur1p converts ceramides into IPC. This conversion probably drives ceramide transport from the ER to the Golgi. We found that Nvj2-dependent ceramide transport to the medial-Golgi decreases ceramide levels, which helps prevent ceramide intoxication. Thus, cells use nonvesicular lipid transport at MCSs to prevent the accumulation of a toxic lipid intermediate (Fig. 10 A). It seems likely that this method is used to prevent the toxic accumulation of lipids in addition to ceramide. Another important function of Nvj2p-faciliated ceramide transport during ER stress may be to allow cells to continue producing sphingolipids when vesicular trafficking is compromised.

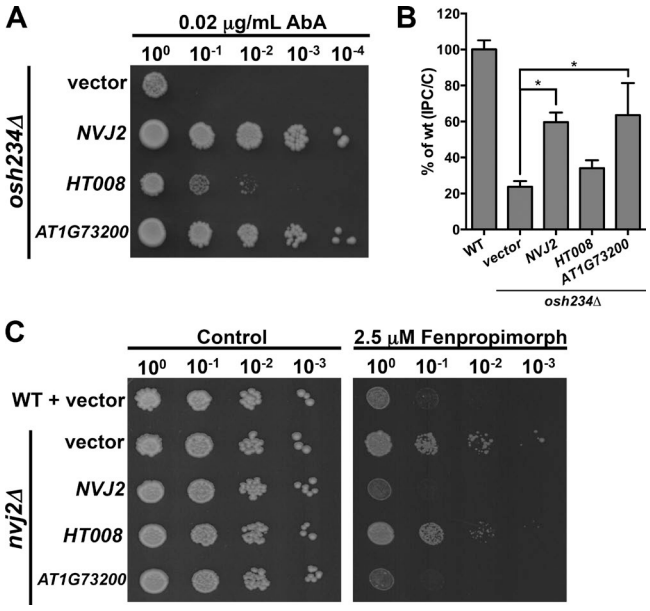

Figure 9. **Nvj2p homologues in higher eukaryotes partially functional in yeast.** (A) Serial dilutions of cultures *osh234Δ* with the indicated plasmids were spotted on plates containing 0.02 µg/ml AbA. (B) Cells were labeled with [^{3}H]serine as in Fig. 1 C. Mean ± SD of five independent experiments. (C) Serial dilutions of cultures of the indicated strains on plates with or without 2.5 µM fenpropimorph. *, P < 0.05, *t* test. WT, wild-type.

Role of Nvj2p in alleviating lipotoxicity

Our findings suggest Nvj2p plays a relatively minor role in facilitating ER to Golgi ceramide transport during normal growth conditions. We found that cells lacking Nvj2p have only an ∼30% reduction in nonvesicular ceramide transport (Fig. 1 I), indicating that Nvj2p is not required for this transport. However, our findings reveal that Nvj2p plays an important role in facilitating lipid exchange between the ER and the Golgi complex during ER stress, when Nvj2p dramatically increases tethering between these organelles. During ER stress, vesicular trafficking may substantially slow or stop, whereas ceramide production continues, which would results in the toxic accumulation of ceramide in the ER if there were not pathways that remove excess ceramide. Some of this ceramide may be degraded by the ceramidases Ydc1p and Ypc1p (Mao et al., 2000a,b). Our findings suggest that yeast has two other mechanisms for removing the excess ceramide: converting it to acylceramide and transferring it to the Golgi complex where it is converted to IPC (Fig. 10 B). These two pathways seem to be redundant because cells lacking only Nvj2p or only the proteins that produce acylceramides (Lro1p and Dga1p) only slightly higher ceramide levels than wild-type cells when treated with DTT to induce ER stress (Fig. 8, I and K). However, cells lacking both pathways have a dramatic ceramide increase during ER stress and grow poorly even in the absence of ER stress, suggesting both pathways prevent the toxic buildup of ceramide (Fig. 8, K–M). Ceramides probably also build to toxic levels in cells lacking Nvj2p that constitutively overproduce ceramides (e.g., *orm1Δ orm2Δ njv2Δ*; Fig. 8, H and I). Thus, Nvj2p-depenent ceramide transport from the ER to the Golgi complex plays a role in preventing the toxic accumulation during ER stress. It seems likely that ER–Golgi tethering by Nvj2p during ER stress also facilitates the exchange of other lipids between these organelles.

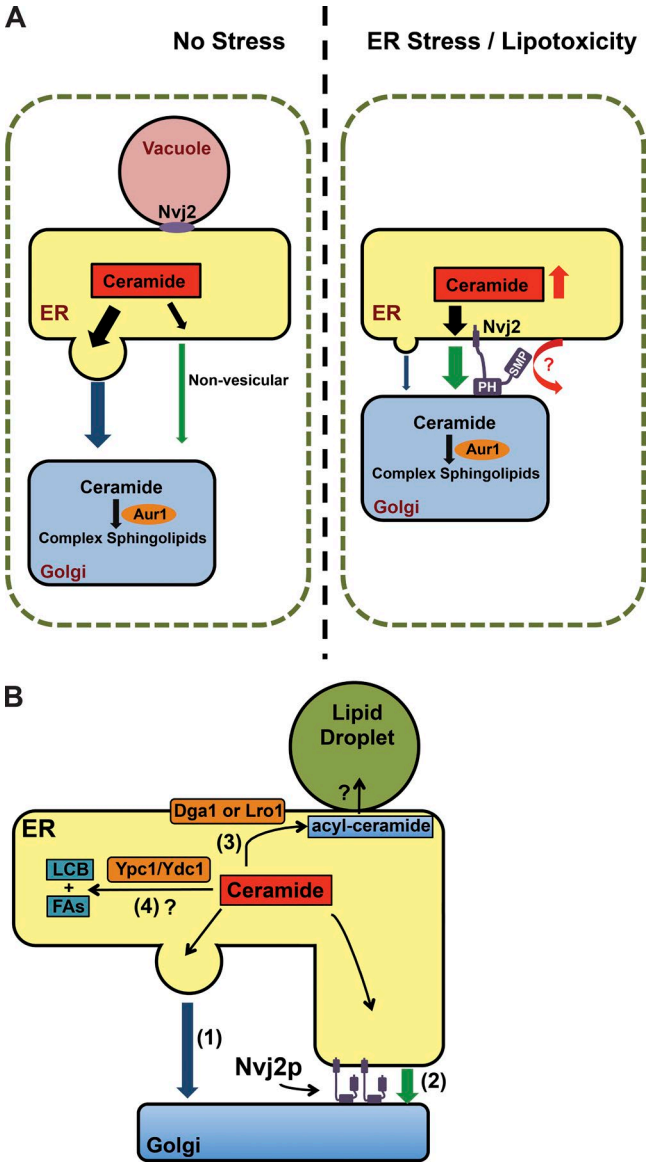

Figure 10. **Models of Nvj2p-dependent ER–medial Golgi tethering during stress and pathways of ceramide removal from the ER.** (A) In the absence of ER stress, Nvj2p is largely at the NVJ and plays a minor role in nonvesicular ceramide transport to the Golgi complex (left panel). During ER stress or ceramide overproduction, Nvj2p relocalizes to and increases ER–medial Golgi contacts, facilitating ceramide exit from the ER. (B) Pathways of ceramide removal from the ER in yeast: vesicular transport (1), Nvj2-dependent nonvesicular transport (2), conversion into acyl-ceramide (3), and perhaps degradation (4). During ER stress, when vesicular trafficking is compromised, Nvj2-dependent ceramide removal from the ER and ceramide acylation play redundant roles in preventing toxic amounts of ceramide from accumulating in the ER. FA, fatty acid.

How does Nvj2p facilitate ceramide transport?

The SMP domain of Nvj2p, which we show is essential for function (Fig. 2 and Fig. S1 A), may bind and transfer ceramides. It has recently been found that the SMP domains of extended synaptotagmins (E-Syts), proteins that reside at contacts between the ER and plasma membrane, transfer glycerolipids between membranes (Saheki et al., 2016; Yu et al., 2016). The SMP domains in the E-Syts can bind a variety of lipids, and the same might be true of the SMP in Nvj2p. We have obtained indirect evidence that the SMP domain in Nvj2p binds lipids. Mutations were generated in the SMP domain of Nvj2p that are similar to mutations in the SMP domain of E-Syt1 that block lipid binding. The mutant Nvj2p fails to transport lipids both in vitro and in cell (Fig. 2, C and D), suggesting that Nvj2p may directly transport ceramide. However, even if Nvj2p directly transports ceramide, other proteins do as well because nonvesicular ceramide transport still occurs in cells lacking Nvj2p. It is also possible that the primary role of Nvj2p in facilitating ceramide transfer to the medial-Golgi is to serve as a tether; we found that the ability of Nvj2p to facilitate ceramide transport to the Golgi is partially complemented by the artificial ER–Golgi tether EGT. Thus, Nvj2p could primarily serve as a tether and ceramide transport could be mediated by several proteins. Something similar may occur in mammalian cells because it has been suggested that several lipid transport proteins work together at ER–Golgi MCSs, and some of these proteins may function as primarily tethers (Peretti et al., 2008; Mesmin et al., 2013; Goto et al., 2016).

Regulation of contact formation by Nvj2p

Understanding how the localization of Nvj2p is regulated is an interesting question for the future. It will be important to understanding how the cytoplasmic domain of Nvj2p can target the protein to both the NVJ and ER–Golgi contacts (and perhaps other MSCs as well). Our results suggest that the PH domain of Nvj2p is required for the protein to bind Golgi membranes but what lipids and/or proteins are bound is not yet known. The signal that causes Nvj2p to relocalize from the NVJ is not known but may be NVJ disassembly, which we find occurs during ER stress (Fig. S2 C). Interestingly, Nvj2p relocation from the NVJ to ER–Golgi contacts during ER stress does not require the kinase Ire1p, the master regulator of the cellular response to ER stress (unpublished data). Cells may have undiscovered mechanisms for sensing and preventing the accumulation of toxic lipids during ER stress.

Regulation of ER–Golgi contact site formation may be significantly different in mammalian cells and in yeast because contacts seem to be constantly present in mammalian cells but only found in yeast cells during stress conditions. One of the only known ER–Golgi tehers in mammalian cells, oxysterol-binding protein, may be constantly at these junctions but becomes enriched there when a lipid it binds accumulates in the Golgi membrane (Mesmin et al., 2013). In contrast, Nvj2p seems to somehow cause de novo tethering during ER stress or when ceramide accumulate in the ER.

Mammalian homologues of Nvj2p

We have previously shown that the human homologue of Nvj2p (HT008) localizes to the NVJ when expressed in yeast (Toulmay and Prinz, 2012), and in this study, we demonstrate that HT008 can partially genetically compensate for the loss of Nvj2p. These findings suggest that HT008, like Nvj2p, may regulate MCS formation during ER stress and may play a role in preventing lipotoxicity. It will be particularly interesting to determine whether HT008 works in concert with CERT to mediate nonvesicular ceramide trafficking in normal growth conditions and during stress. Understanding how cells modulate lipid exchange at MCSs to regulate lipid metabolism and prevent lipotoxicity is an important challenge for the future.

Materials and methods

Strains, plasmids, and growth media

The plasmids and strains used are listed in Tables S2 and S3. Media used were YPD (1% yeast extract, 2% peptone, and 2% glucose) and synthetic complete (SC) media (2% glucose, 0.67% yeast nitrogen base without amino acids, and amino acid dropout mix). Strains were constructed using standard methods.

Yeast growth plating assay

Strains were grown at 30°C to mid-logarithmic growth phase in SC medium. The cells were collected, and 1.5 OD_{600} of each culture was spotted in four 10-fold dilutions on SC plates with the indicated compounds and incubated at 30°C for 3 d.

In vivo labeling to measure conversion of ceramide to IPC

To measure the conversion of ceramide to IPC, cells were labeled with [^{3}H]serine (American Radiolabeled Chemicals, Inc.) as previously described (Kajiwara et al., 2008, 2014) with the following modifications. In brief, 20 µCi [^{3}H]serine was added to 10 OD_{600} of cultures in mid-logarithmic growth phase in SC without serine at 25°C, and the cells were grown for 1 h. For experiments with strains containing the temperature-sensitive *sec18-1* allele, cells were initially grown at 25°C, 200 µg/ml cycloheximide was added to the medium, the cells were grown for 20 more minutes at 25°C, the culture was shifted to 37°C for 30 min, and then labeled for 30 min with 20 µCi [^{3}H]serine (Funato and Riezman, 2001). After labeling, growth was stopped by addition of 10 mM NaF and 10 mM NaN_3 and placing cultures on ice for 20 min. The cells were washed with water, and lipids were extracted and subjected to mild alkaline hydrolysis to deacylate glycophospholipids as described (Kajiwara et al., 2008, 2014). Lipids were dried under nitrogen and separated on silica TLC plates (EMD Millipore) using the chloroform/methanol/4.2 N ammonium hydroxide (9:7:2). TLC plates were scanned on a RITA* Thin Layer Analyzer (Raytest) to quantify radiolabeled lipids and determine the ratio of IPC to ceramide.

Measurement of ceramide and IPC levels

Ceramide levels were measured as described (Puoti et al., 1991). In brief, 10 OD_{600} of cells in mid-logarithmic growth phase in SC were labeled with 5 µCi [^{3}H]palmitic acid (American Radiolabeled Chemicals, Inc.) for 4 h. After labeling, the cells were harvested, and lipids were extracted and subjected to mild-alkaline hydrolysis as described (Kajiwara et al., 2008, 2014). The lipids were applied to silica TLC plates and resolved with chloroform/methanol/2 M ammonium hydroxide (40:10:1). The TLC plates were scanned (see In vivo labeling to measure conversion of ceramide to IPC), and the amount of ceramide detected was normalized to the total amount of radiolabeled lipid in each sample. To determine IPC production, cells were labeled with [^{3}H]serine for 1 h and processed as described in the previous section. It should be noted that with this labeling condition, very little mannosyl-inositolphosphorylceramide or mannosyl-diinositolphosphorylceramide was formed.

In vitro labeling of lysates with [^{3}H]DHS

Labeling of cell lysates with [^{3}H]DHS (from T. Futerman, Weizmann Institute of Sciences, Rehovot, Israel) was performed as previously described (Funato and Riezman, 2001) with the following modifications. Cell from cultures in mid-logarithmic growth phase in SC medium were harvested, and ∼100 OD600 of cells was resuspended in 15 ml of 100 mM Tris-HCl, pH 9.4, and incubated at 30°C for 10 min. The cells were washed and resuspended in 7.5 ml of 0.2× YPD, 0.6 M sorbitol, 10 mM KPi, pH 7.5, with 2.25 mg zymolyase 20T (AMS BIO). After incubation for 20 min at 30°C, the cells were washed and resuspended in ice-cold lysis buffer (0.2 M sorbitol, 50 mM KOAc, 20 mM Hepes, pH 6.8, and 2 mM EDTA and protease inhibitors). The resulting spheroplasts were lysed with a dounce homogenizer using a tight pestle. Debris and unlysed cells were removed by centrifugation at 500 *g* for 10 min at 4°C. The labeling reactions contained 100–200 µg lysate, ATP-regenerating system (1 mM ATP, 40 mM phosphocreatine, 0.2 mg/ml creatine phosphokinase, 20 mM $MgCl_2$, 20 mM Tris-HCl, pH 7.2, and 1 mM β-ME), 30 µM [^{3}H]DHS (0.5 µCi), 50 µM hexacosanoyl Coenzyme A (C26:0; Avanti Polar Lipids, Inc.), and 20 µM BSA in lysis buffer in a total volume of 100 µl. When MBP fusions or MBP were added to the reactions, the buffer also contained 0.1% Mega-8. After incubation a 25°C for 2 h, the reactions were stopped with 600 µl chloroform/methanol (1:1). The organic phase was collected and reextracted with 400 µl chloroform/methanol/H_2O (20:20:6). Lipids were dried under nitrogen, applied to silica TLC plates, and resolved using chloroform/methanol/4.2 N ammonium hydroxide (9:7:2) to quantitate IPC or solvent system chloroform/methanol/2 M ammonium hydroxide (40:10:1) to quantitate ceramide.

Fluorescence microscopy

Cells in mid-logarithmic growth phase SC were visualized live the growth medium using a BX61 microscope (Olympus) with an UPlan Apo 1006/1.35 NA lens, a camera (Retiga EX; QImaging), and IVision software (version 4.0.5; BioVision Technologies). To induce ER stress before visualization, 10 mM DTT was added to the medium, and the cells were grown for 4 h.

EM

Sample preparation for EM was done as described previously (Choudhary et al., 2015). Cells were grown to mid-logarithmic growth phase at 30°C, samples were treated with and without 10 mM DTT and incubated for additional 4 h at 30°C with shaking. Cells corresponding to 10 OD_{600} were harvested at 2000 rpm for 5 min. The cell pellet was resuspended in 2.5 ml fixative media (2.5% glutaraldehyde [Electron Microscopy Sciences], 1.25% PFA, and 40 mM potassium phosphate, pH 7.0) for 20 min at RT. Cells were harvested and again resuspended in 2.5 ml fresh fixative media and incubated on ice for 1 h. Cells were centrifuged and washed twice with 0.9% NaCl and once with water. Cells were resuspended with 2% solution of $KMnO_4$ for 5 min at RT, centrifuged, and again incubated with fresh solution of 2% $KMnO_4$ for 45 min at RT for en bloc staining. The cells were dehydrated using graded series of ethanol, embedded using Spurr's resin (Electron Microscopy Sciences), and polymerized at 60°C for 2 to 3 d. Ultrathin sections (70 nm) were produced using a diamond knife (Diatome AG) on an ultra-microtome (Ultracut UCT; Leica Biosystems), collected on 200 mesh formvar-coated copper grids (Electron Microscopy Sciences), poststained with uranyl acetate and lead citrate, air dried, and visualized with a transmission EM (Tecnai T12; Thermo Fisher Scientific) operating at 120 kV. Pictures were recorded on a below-mounted 2k × 2k CCD camera (Gatan, Inc.). Brightness and contrast were adjusted to the entire images using Photoshop (version CC 2014; Adobe Systems).

Imaging of cells expressing Aur1-GFP-APEX2

The gene encoding APEX2 (Martell et al., 2012; Lam et al., 2015) was cloned into a plasmid expressing Aur1-GFP-APEX2 under the *AUR1* promoter. Strains containing this plasmid were grown to mid-logarithmic growth phase at 30°C in a SC medium. Where indicated, 10 mM DTT was added to the medium, and cultures were grown for 4 h at 30°C with shaking. Cells corresponding to 10 OD_{600} were harvested and overlaid with fixative (2.5% glutaraldehyde, 1.25% PFA, and 0.1 M sodium cacodylate buffer, pH 7.4; Electron Microscopy Sciences) for

30 min at RT to generate EM contrast and subsequently resuspended in fresh fixative and incubated on ice for 30 min. The method to visualize APEX2 was adapted as described previously (Martell et al., 2012; Ariotti et al., 2015; Lam et al., 2015). Cells were washed three times in 0.1 M sodium cacodylate buffer to remove glutaraldehyde. A DAB solution was made by dissolving tablets (Sigma-Aldrich) into sodium cacodylate buffer (0.1 M, pH 7.4) so that the final concentration of DAB was 1 mg/ml. The solution was filtered using a 0.2-µm filter (EMD Millipore) to remove insoluble precipitate. The tube in which DAB solution was prepared was wrapped with aluminum foil. Cells were overlaid with 2 ml DAB solution and incubated in the dark for 10 min at RT, harvested, resuspended into fresh DAB solution containing 10 mM H_2O_2 (Sigma-Aldrich), and reincubated in the dark for another 30 min at RT to produce the insoluble reaction product. Cells were rinsed three times with 0.1 M sodium cacodylate buffer, pH 7.4, and postfixed with 1% OsO_4 (Electron Microscopy Sciences) in 0.1 M sodium cacodylate buffer, pH 7.4, for 30 min at RT. Subsequently, cells were washed three times with 0.1 M sodium cacodylate buffer, pH 7.4, and two times with distilled H_2O. Cells were dehydrated using a graded series of ethanol, embedded using resin (EMBed 812; Electron Microscopy Sciences), and polymerized as described in the previous section. Ultrathin sections (50–60 nm) were produced using an ultra-microtome (Ultracut UCT; Leica Biosystems) and visualized without poststaining with a transmission EM (Tecnai T12; Thermo Fisher Scientific) operating at 120 kV.

Unfolding protein response assay

Cells were transformed with pMCZ-Y, a plasmid expressing the lacZ gene under the *KAR2* promoter. To induce an unfolding protein response, 8 mM DTT was added to cultures of growing cells for 1 h. The β-galactosidase activity of the cultures assay was determined as described (Pagani et al., 2000).

Cell death assays

The assay was performed as described (Rego et al., 2012). In brief, strains were grown at 30°C in to logarithmic growth phase (OD_{600} = 0.5–0.6) in an SC medium containing 2% galactose instead of glucose. The cells were washed and resuspended in the same medium containing 180 mM acetic acid (Sigma-Aldrich). Cultures were grown at 30°C, and cell viability was assessed at the indicate times by plating on YPD.

Purification of MBP fusions

The genes encoding MBP or MBP fusions were cloned into p416-GAL1 (Mumberg et al., 1994) and expressed in yeast. About 16,000 OD_{600} of cells in 100 ml lysis buffer (500 mM NaCl, 20 mM Tris, pH 7.4, 1 mM EDTA, 1 mM DTT, and protease inhibitors) were lysed with a high-pressure cell disruptor (Constant Systems Limited). The lysate was cleared by centrifugation at 10,000 *g* for 10 min 4°C, filtered, and passed through a column containing amylose (New England Biolabs, Inc.). The column was washed with 500 mM NaCl, 20 mM Tris, pH 7.4, 1 mM EDTA, 1 mM DTT, and 0.1% Mega-8 and eluted with 10 mM maltose, 500 mM NaCl, 20 mM Tris, pH 7.4, 1 mM EDTA, 1 mM DTT, and 0.1% Mega-8.

Preparation of liposomes

Lipids from stock solutions were mixed and dried under N_2 overnight. The lipids were resuspended at 1 mM in either light liposome buffer (20 mM Hepes, pH 7.4, and 100 mM NaCl) or heavy liposome buffer (20 mM Hepes, pH 7.4, and 180 mM sucrose) and vortexed every 15 min for at least 1 h at RT. They then underwent eight cycles of freeze/thaw and were extruded through 0.4-µm pore-size membranes at least 16 times. The heavy liposomes were washed with light liposome buffer and resuspended with light liposome buffer. The light liposomes were cleared by centrifugation at 16,000 *g* for 10 min at 4°C.

Tethering assay

Liposomes were prepared with lipids from Avanti Polar Lipids, Inc.: egg phosphatidylcholine (PC), 18:0–18:1 phosphatidylethanolamine (PE), brain phosphatidylserine (PS), liver PI, egg PA, and 1,2-dioleoyl-sn-glycero-3-[(*N*-(5-amino-1-carboxypentyl)iminodiacetic acid)succinyl] (DGS-NTA[Ni] [nickel salt]). Heavy liposomes contained PC/PE/DGS-NTA(Ni) (75:20:5). Light liposomes contained PC/PI/PE/PS (45:20:20:10) and 5 mol% of PA, phosphatidylinositol 3-phosphate, PC, or phosphatidylinositol 4-phosphate or 2.5 mol% of either phosphatidylinositol 3,5-bisphosphate or phosphatidylinositol 4,5-bisphosphate and 2.5 mol% PC. The light liposomes also contained a trace amount of [^{3}H]triolein (American Radiolabeled Chemicals, Inc.). Each tethering assay had 45 µl light liposomes, 45 µl heavy liposomes or light liposome buffer, 10 µl (100 pmol) protein or buffer, and 10 µl of 1% Mega-8. The samples were incubated at 30°C for 1 h, placed on ice, and centrifuged at 16,000 *g* for 10 min at 4°C. The supernatant (80 µl) was counted using a scintillation counter. The percentage of light liposomes pelleted was calculated from the percentage of remaining in the supernatant.

Online supplemental material

Fig. S1 contains additional data related to Fig. 1 showing that all three domains of Nvj2p are required for it to confer resistance to AbA in *osh234Δ* cells, the localization of Aur1p does not change in cells overexpressing Nvj2p, the expression of Aur1p does not change in cells overexpressing Nvj2p, and control for experiments in Fig. 1, H–J. Fig. S2 contains additional data related to Figs. 2, 3, and 4 showing that the Nvj2-GFP mutants were expressed at levels similar to Nvj2-GFP, the expression of Nvj2p does not change when cells are treated with DTT, the localization of Nvj1-GFP or GFP-Osh1 during ER stress, the PH domain of Nvj2p is necessary to target Nvj2p to Golgi membranes, and a scheme of the tethering assay shown in Fig. 3 D. Fig. S3 contains additional data related to Fig. 5 showing that DAB staining does not produce contrast in cells that do not express APEX2, Nvj2p overexpression increases contact between the ER, and vesicles that are likely medial-Golgi. Fig. S4 contains additional data related to Fig. 6 showing that EGT colocalizes with cis- and medial-Golgi, Aur1-mKate localization is not altered by EGT expression, and lysates from cell either with or without EGT produce similar amounts of ceramide. Fig. S5 contains additional data related to Figs. 7 and 8 showing that the localization of *Nvj1(1–120)-Nvj2ΔTM-GFP* does not change in cells treated with DTT, that cells that overproduce ceramide are hypersensitive to tunicamycin, and Nvj2p is probably not a negative regulator of serine palmitoyltransferase. Table S1 lists the plasmids obtained from a high-copy library that allow *osh234Δ* cells to grow in the presence of AbA. Tables S2 and S3 list the plasmids and strains used in this study.

Acknowledgments

We thank Tony Futerman, Yihong Ye, Amy Chang, Christopher Burd, Tim Levine, François Doignon, and Christopher Beh for providing materials and Tom Rapoport for critically reading the manuscript.

This work was supported by the Intramural Research Program of the National Institute of Diabetes and Digestive and Kidney Diseases.

The authors declare no competing financial interests.

Submitted: 10 June 2016
Revised: 20 October 2016
Accepted: 7 December 2016

References

AhYoung, A.P., J. Jiang, J. Zhang, X. Khoi Dang, J.A. Loo, Z.H. Zhou, and P.F. Egea. 2015. Conserved SMP domains of the ERMES complex bind phospholipids and mediate tether assembly. *Proc. Natl. Acad. Sci. USA*. 112:E3179–E3188. http://dx.doi.org/10.1073/pnas.1422363112

Ariotti, N., T.E. Hall, J. Rae, C. Ferguson, K.A. McMahon, N. Martel, R.E. Webb, R.I. Webb, R.D. Teasdale, and R.G. Parton. 2015. Modular detection of GFP-labeled proteins for rapid screening by electron microscopy in cells and organisms. *Dev. Cell.* 35:513–525. http://dx.doi.org/10.1016/j.devcel.2015.10.016

Bikman, B.T., and S.A. Summers. 2011. Ceramides as modulators of cellular and whole-body metabolism. *J. Clin. Invest.* 121:4222–4230. http://dx.doi.org/10.1172/JCI57144

Breslow, D.K., S.R. Collins, B. Bodenmiller, R. Aebersold, K. Simons, A. Shevchenko, C.S. Ejsing, and J.S. Weissman. 2010. Orm family proteins mediate sphingolipid homeostasis. *Nature.* 463:1048–1053. http://dx.doi.org/10.1038/nature08787

Cerantola, V., I. Guillas, C. Roubaty, C. Vionnet, D. Uldry, J. Knudsen, and A. Conzelmann. 2009. Aureobasidin A arrests growth of yeast cells through both ceramide intoxication and deprivation of essential inositolphosphorylceramides. *Mol. Microbiol.* 71:1523–1537. http://dx.doi.org/10.1111/j.1365-2958.2009.06628.x

Choudhary, V., N. Ojha, A. Golden, and W.A. Prinz. 2015. A conserved family of proteins facilitates nascent lipid droplet budding from the ER. *J. Cell Biol.* 211:261–271. http://dx.doi.org/10.1083/jcb.201505067

De Matteis, M.A., and L.R. Rega. 2015. Endoplasmic reticulum-Golgi complex membrane contact sites. *Curr. Opin. Cell Biol.* 35:43–50. http://dx.doi.org/10.1016/j.ceb.2015.04.001

Dickson, R.C., and R.L. Lester. 1999. Metabolism and selected functions of sphingolipids in the yeast *Saccharomyces cerevisiae*. *Biochim. Biophys. Acta.* 1438:305–321. http://dx.doi.org/10.1016/S1388-1981(99)00068-2

Eisenberg, T., and S. Büttner. 2014. Lipids and cell death in yeast. *FEMS Yeast Res.* 14:179–197. http://dx.doi.org/10.1111/1567-1364.12105

Funato, K., and H. Riezman. 2001. Vesicular and nonvesicular transport of ceramide from ER to the Golgi apparatus in yeast. *J. Cell Biol.* 155:949–959. http://dx.doi.org/10.1083/jcb.200105033

Gallego, O., M.J. Betts, J. Gvozdenovic-Jeremic, K. Maeda, C. Matetzki, C. Aguilar-Gurrieri, P. Beltran-Alvarez, S. Bonn, C. Fernández-Tornero, L.J. Jensen, et al. 2010. A systematic screen for protein-lipid interactions in *Saccharomyces cerevisiae*. *Mol. Syst. Biol.* 6:430. http://dx.doi.org/10.1038/msb.2010.87

Goto, A., M. Charman, and N.D. Ridgway. 2016. Oxysterol-binding protein activation at endoplasmic reticulum-Golgi contact sites reorganizes phosphatidylinositol 4-phosphate pools. *J. Biol. Chem.* 291:1336–1347. http://dx.doi.org/10.1074/jbc.M115.682997

Graham, T.R., and S.D. Emr. 1991. Compartmental organization of Golgi-specific protein modification and vacuolar protein sorting events defined in a yeast sec18 (NSF) mutant. *J. Cell Biol.* 114:207–218. http://dx.doi.org/10.1083/jcb.114.2.207

Han, S., M.A. Lone, R. Schneiter, and A. Chang. 2010. Orm1 and Orm2 are conserved endoplasmic reticulum membrane proteins regulating lipid homeostasis and protein quality control. *Proc. Natl. Acad. Sci. USA*. 107:5851–5856. http://dx.doi.org/10.1073/pnas.0911617107

Hanada, K., K. Kumagai, S. Yasuda, Y. Miura, M. Kawano, M. Fukasawa, and M. Nishijima. 2003. Molecular machinery for non-vesicular trafficking of ceramide. *Nature.* 426:803–809. http://dx.doi.org/10.1038/nature02188

Hjelmqvist, L., M. Tuson, G. Marfany, E. Herrero, S. Balcells, and R. Gonzàlez-Duarte. 2002. ORMDL proteins are a conserved new family of endoplasmic reticulum membrane proteins. *Genome Biol.* 3:H0027. http://dx.doi.org/10.1186/gb-2002-3-6-research0027

Holland, W.L., J.T. Brozinick, L.P. Wang, E.D. Hawkins, K.M. Sargent, Y. Liu, K. Narra, K.L. Hoehn, T.A. Knotts, A. Siesky, et al. 2007. Inhibition of ceramide synthesis ameliorates glucocorticoid-, saturated-fat-, and obesity-induced insulin resistance. *Cell Metab.* 5:167–179. http://dx.doi.org/10.1016/j.cmet.2007.01.002

Ito, M., N. Okino, and M. Tani. 2014. New insight into the structure, reaction mechanism, and biological functions of neutral ceramidase. *Biochim. Biophys. Acta.* 1841:682–691. http://dx.doi.org/10.1016/j.bbalip.2013.09.008

Kajiwara, K., R. Watanabe, H. Pichler, K. Ihara, S. Murakami, H. Riezman, and K. Funato. 2008. Yeast ARV1 is required for efficient delivery of an early GPI intermediate to the first mannosyltransferase during GPI assembly and controls lipid flow from the endoplasmic reticulum. *Mol. Biol. Cell.* 19:2069–2082. http://dx.doi.org/10.1091/mbc.E07-08-0740

Kajiwara, K., A. Ikeda, A. Aguilera-Romero, G.A. Castillon, S. Kagiwada, K. Hanada, H. Riezman, M. Muñiz, and K. Funato. 2014. Osh proteins regulate COPII-mediated vesicular transport of ceramide from the endoplasmic reticulum in budding yeast. *J. Cell Sci.* 127:376–387. http://dx.doi.org/10.1242/jcs.132001

Kim, S.K., Y.H. Noh, J.R. Koo, and H.S. Yun. 2010. Effect of expression of genes in the sphingolipid synthesis pathway on the biosynthesis of ceramide in *Saccharomyces cerevisiae*. *J. Microbiol. Biotechnol.* 20:356–362.

Kornmann, B., E. Currie, S.R. Collins, M. Schuldiner, J. Nunnari, J.S. Weissman, and P. Walter. 2009. An ER-mitochondria tethering complex revealed by a synthetic biology screen. *Science.* 325:477–481. http://dx.doi.org/10.1126/science.1175088

Kumagai, K., M. Kawano, F. Shinkai-Ouchi, M. Nishijima, and K. Hanada. 2007. Interorganelle trafficking of ceramide is regulated by phosphorylation-dependent cooperativity between the PH and START domains of CERT. *J. Biol. Chem.* 282:17758–17766. http://dx.doi.org/10.1074/jbc.M702291200

Kurokawa, K., M. Okamoto, and A. Nakano. 2014. Contact of cis-Golgi with ER exit sites executes cargo capture and delivery from the ER. *Nat. Commun.* 5:3653. http://dx.doi.org/10.1038/ncomms4653

Kvam, E., and D.S. Goldfarb. 2006. Structure and function of nucleus-vacuole junctions: Outer-nuclear-membrane targeting of Nvj1p and a role in tryptophan uptake. *J. Cell Sci.* 119:3622–3633. http://dx.doi.org/10.1242/jcs.03093

Lam, S.S., J.D. Martell, K.J. Kamer, T.J. Deerinck, M.H. Ellisman, V.K. Mootha, and A.Y. Ting. 2015. Directed evolution of APEX2 for electron microscopy and proximity labeling. *Nat. Methods.* 12:51–54. http://dx.doi.org/10.1038/nmeth.3179

Ledeen, R.W., and G. Wu. 2008. Nuclear sphingolipids: Metabolism and signaling. *J. Lipid Res.* 49:1176–1186. http://dx.doi.org/10.1194/jlr.R800009-JLR200

Levine, T.P., C.A. Wiggins, and S. Munro. 2000. Inositol phosphorylceramide synthase is located in the Golgi apparatus of *Saccharomyces cerevisiae*. *Mol. Biol. Cell.* 11:2267–2281. http://dx.doi.org/10.1091/mbc.11.7.2267

Liu, M., C. Huang, S.R. Polu, R. Schneiter, and A. Chang. 2012. Regulation of sphingolipid synthesis through Orm1 and Orm2 in yeast. *J. Cell Sci.* 125:2428–2435. http://dx.doi.org/10.1242/jcs.100578

Mao, C., R. Xu, A. Bielawska, and L.M. Obeid. 2000a. Cloning of an alkaline ceramidase from *Saccharomyces cerevisiae*. An enzyme with reverse (CoA-independent) ceramide synthase activity. *J. Biol. Chem.* 275:6876–6884. http://dx.doi.org/10.1074/jbc.275.10.6876

Mao, C., R. Xu, A. Bielawska, Z.M. Szulc, and L.M. Obeid. 2000b. Cloning and characterization of a *Saccharomyces cerevisiae* alkaline ceramidase with specificity for dihydroceramide. *J. Biol. Chem.* 275:31369–31378. http://dx.doi.org/10.1074/jbc.M003683200

Martell, J.D., T.J. Deerinck, Y. Sancak, T.L. Poulos, V.K. Mootha, G.E. Sosinsky, M.H. Ellisman, and A.Y. Ting. 2012. Engineered ascorbate peroxidase as a genetically encoded reporter for electron microscopy. *Nat. Biotechnol.* 30:1143–1148. http://dx.doi.org/10.1038/nbt.2375

Martínez-Montañés, F., and R. Schneiter. 2016. Following the flux of long-chain bases through the sphingolipid pathway in vivo using mass spectrometry. *J. Lipid Res.* 57:906–915. http://dx.doi.org/10.1194/jlr.D066472

Megyeri, M., H. Riezman, M. Schuldiner, and A.H. Futerman. 2016. Making sense of the yeast sphingolipid pathway. *J. Mol. Biol.* 428:4765–4775. http://dx.doi.org/10.1016/j.jmb.2016.09.010

Merrill, A.H. Jr. 2002. De novo sphingolipid biosynthesis: A necessary, but dangerous, pathway. *J. Biol. Chem.* 277:25843–25846. http://dx.doi.org/10.1074/jbc.R200009200

Mesmin, B., J. Bigay, J. Moser von Filseck, S. Lacas-Gervais, G. Drin, and B. Antonny. 2013. A four-step cycle driven by PI(4)P hydrolysis directs sterol/PI(4)P exchange by the ER-Golgi tether OSBP. *Cell.* 155:830–843. http://dx.doi.org/10.1016/j.cell.2013.09.056

Michaelson, L.V., J.A. Napier, D. Molino, and J.D. Faure. 2016. Plant sphingolipids: Their importance in cellular organization and adaption. *Biochim. Biophys. Acta.* 1861:1329–1335. http://dx.doi.org/10.1016/j.bbalip.2016.04.003

Mullen, T.D., and L.M. Obeid. 2012. Ceramide and apoptosis: Exploring the enigmatic connections between sphingolipid metabolism and programmed cell death. *Anticancer. Agents Med. Chem.* 12:340–363. http://dx.doi.org/10.2174/187152012800228661

Mumberg, D., R. Müller, and M. Funk. 1994. Regulatable promoters of *Saccharomyces cerevisiae*: Comparison of transcriptional activity and their use for heterologous expression. *Nucleic Acids Res.* 22:5767–5768. http://dx.doi.org/10.1093/nar/22.25.5767

Pagani, M., M. Fabbri, C. Benedetti, A. Fassio, S. Pilati, N.J. Bulleid, A. Cabibbo, and R. Sitia. 2000. Endoplasmic reticulum oxidoreductin 1-lbeta (ERO1-Lbeta), a human gene induced in the course of the unfolded protein response. *J. Biol. Chem.* 275:23685–23692. http://dx.doi.org/10.1074/jbc.M003061200

Pan, X., P. Roberts, Y. Chen, E. Kvam, N. Shulga, K. Huang, S. Lemmon, and D.S. Goldfarb. 2000. Nucleus-vacuole junctions in *Saccharomyces cerevisiae* are formed through the direct interaction of Vac8p with Nvj1p. *Mol. Biol. Cell.* 11:2445–2457. http://dx.doi.org/10.1091/mbc.11.7.2445

Peretti, D., N. Dahan, E. Shimoni, K. Hirschberg, and S. Lev. 2008. Coordinated lipid transfer between the endoplasmic reticulum and the Golgi complex requires the VAP proteins and is essential for Golgi-mediated transport. *Mol. Biol. Cell.* 19:3871–3884. http://dx.doi.org/10.1091/mbc.E08-05-0498

Pickersgill, L., G.J. Litherland, A.S. Greenberg, M. Walker, and S.J. Yeaman. 2007. Key role for ceramides in mediating insulin resistance in human muscle cells. *J. Biol. Chem.* 282:12583–12589. http://dx.doi.org/10.1074/jbc.M611157200

Puoti, A., C. Desponds, and A. Conzelmann. 1991. Biosynthesis of mannosylinositolphosphoceramide in *Saccharomyces cerevisiae* is dependent on genes controlling the flow of secretory vesicles from the endoplasmic reticulum to the Golgi. *J. Cell Biol.* 113:515–525. http://dx.doi.org/10.1083/jcb.113.3.515

Rego, A., M. Costa, S.R. Chaves, N. Matmati, H. Pereira, M.J. Sousa, P. Moradas-Ferreira, Y.A. Hannun, V. Costa, and M. Côrte-Real. 2012. Modulation of mitochondrial outer membrane permeabilization and apoptosis by ceramide metabolism. *PLoS One.* 7:e48571. http://dx.doi.org/10.1371/journal.pone.0048571

Rubio, C., D. Pincus, A. Korennykh, S. Schuck, H. El-Samad, and P. Walter. 2011. Homeostatic adaptation to endoplasmic reticulum stress depends on Ire1 kinase activity. *J. Cell Biol.* 193:171–184. http://dx.doi.org/10.1083/jcb.201007077

Saheki, Y., X. Bian, C.M. Schauder, Y. Sawaki, M.A. Surma, C. Klose, F. Pincet, K.M. Reinisch, and P. De Camilli. 2016. Control of plasma membrane lipid homeostasis by the extended synaptotagmins. *Nat. Cell Biol.* 18:504–515. http://dx.doi.org/10.1038/ncb3339

Schauder, C.M., X. Wu, Y. Saheki, P. Narayanaswamy, F. Torta, M.R. Wenk, P. De Camilli, and K.M. Reinisch. 2014. Structure of a lipid-bound extended synaptotagmin indicates a role in lipid transfer. *Nature.* 510:552–555. http://dx.doi.org/10.1038/nature13269

Schneiter, R. 1999. Brave little yeast, please guide us to thebes: Sphingolipid function in *S. cerevisiae*. *BioEssays.* 21:1004–1010. http://dx.doi.org/10.1002/(SICI)1521-1878(199912)22:1<1004::AID-BIES4>3.0.CO;2-Y

Schorling, S., B. Vallée, W.P. Barz, H. Riezman, and D. Oesterhelt. 2001. Lag1p and Lac1p are essential for the Acyl-CoA-dependent ceramide synthase reaction in *Saccharomyces cerevisae*. *Mol. Biol. Cell.* 12:3417–3427. http://dx.doi.org/10.1091/mbc.12.11.3417

Shimobayashi, M., W. Oppliger, S. Moes, P. Jenö, and M.N. Hall. 2013. TORC1-regulated protein kinase Npr1 phosphorylates Orm to stimulate complex sphingolipid synthesis. *Mol. Biol. Cell.* 24:870–881. http://dx.doi.org/10.1091/mbc.E12-10-0753

Tafesse, F.G., A.M. Vacaru, E.F. Bosma, M. Hermansson, A. Jain, A. Hilderink, P. Somerharju, and J.C. Holthuis. 2014. Sphingomyelin synthase-related protein SMSr is a suppressor of ceramide-induced mitochondrial apoptosis. *J. Cell Sci.* 127:445–454. http://dx.doi.org/10.1242/jcs.138933

Ternes, P., J.F. Brouwers, J. van den Dikkenberg, and J.C. Holthuis. 2009. Sphingomyelin synthase SMS2 displays dual activity as ceramide phosphoethanolamine synthase. *J. Lipid Res.* 50:2270–2277. http://dx.doi.org/10.1194/jlr.M900230-JLR200

Toulmay, A., and W.A. Prinz. 2012. A conserved membrane-binding domain targets proteins to organelle contact sites. *J. Cell Sci.* 125:49–58. http://dx.doi.org/10.1242/jcs.085118

Vacaru, A.M., F.G. Tafesse, P. Ternes, V. Kondylis, M. Hermansson, J.F. Brouwers, P. Somerharju, C. Rabouille, and J.C. Holthuis. 2009. Sphingomyelin synthase-related protein SMSr controls ceramide homeostasis in the ER. *J. Cell Biol.* 185:1013–1027. http://dx.doi.org/10.1083/jcb.200903152

Voynova, N.S., C. Vionnet, C.S. Ejsing, and A. Conzelmann. 2012. A novel pathway of ceramide metabolism in *Saccharomyces cerevisiae*. *Biochem. J.* 447:103–114. http://dx.doi.org/10.1042/BJ20120712

Xie, Z., M. Fang, M.P. Rivas, A.J. Faulkner, P.C. Sternweis, J.A. Engebrecht, and V.A. Bankaitis. 1998. Phospholipase D activity is required for suppression of yeast phosphatidylinositol transfer protein defects. *Proc. Natl. Acad. Sci. USA.* 95:12346–12351. http://dx.doi.org/10.1073/pnas.95.21.12346

Yu, H., Y. Liu, D.R. Gulbranson, A. Paine, S.S. Rathore, and J. Shen. 2016. Extended synaptotagmins are Ca2+-dependent lipid transfer proteins at membrane contact sites. *Proc. Natl. Acad. Sci. USA.* 113:4362–4367. http://dx.doi.org/10.1073/pnas.1517259113

Yu, J.W., J.M. Mendrola, A. Audhya, S. Singh, D. Keleti, D.B. DeWald, D. Murray, S.D. Emr, and M.A. Lemmon. 2004. Genome-wide analysis of membrane targeting by *S. cerevisiae* pleckstrin homology domains. *Mol. Cell.* 13:677–688. http://dx.doi.org/10.1016/S1097-2765(04)00083-8